GEF4610 - DYNAMIC OCEANOGRAPHY:

Waves and wave-induced mass transport in the ocean

JAN ERIK H. WEBER

Department of Geosciences

Section for Meteorology and Oceanography

University of Oslo

E-mail: j.e.weber@geo.uio.no

Autumn 2014

CONTENTS

I. GOVERNING EQUATIONS FOR THE OCEAN

1.1 Momentum and mass conservation

We study motion in an ocean with density ρ. The ocean is rotating about the *z*-axis with constant angular velocity $\Omega\sin\varphi$, where φ is the latitude and Ω is the angular velocity of the earth (assumed constant here). Furthermore, (*x*, *y*) are horizontal coordinate axes along the undisturbed sea surface, and the *z*-axis is directed upwards. The respective unit vectors are $(\vec{i},\vec{j},\vec{k})$. The position of the free surface is given by $z=\eta(x,y,t)$, where η is referred to as the surface elevation, and *t* is time. The atmospheric pressure at the surface is denoted by $P_S(x,y,t)$. The bottom topography does not vary with time, and is given by $z=-H(x,y)$; see the sketch in Fig. 1.1.

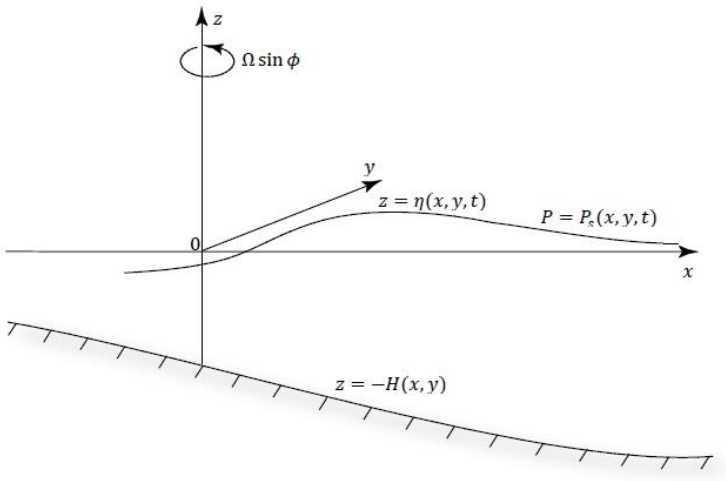

Fig 1.1 *Definition sketch.*

The velocity in the fluid is $\vec{v}=(u,v,w)$, and the pressure is *p*. The momentum equation in a frame of reference fixed to the earth can then be written

$$\frac{D\vec{v}}{dt}\equiv\frac{\partial\vec{v}}{\partial t}+\vec{v}\cdot\nabla\vec{v}=-f\vec{k}\times\vec{v}-\frac{1}{\rho}\nabla p-g\vec{k}+\vec{F}(\vec{v}), \qquad (1.1.1)$$

where $\nabla \equiv \vec{i}\,\partial/\partial x + \vec{j}\,\partial/\partial y + \vec{k}\,\partial/\partial z$ is the gradient operator. Furthermore, g is the acceleration due to gravity, and $f = 2\Omega\sin\varphi$ is the Coriolis parameter. In (1.1.1) we have neglected the horizontal component of the Coriolis force, the tidal force, and the effect of the centrifugal force (due to the earth's rotation) on the apparent gravity. If we let the y-axis point northwards, f is only a function of y. We may then write approximately that

$$f = f_0 + \left(\frac{df}{dy}\right)_0 y = f_0 + \beta y, \tag{1.1.2}$$

where

$$\left.\begin{aligned} f_0 &= 2\Omega\sin\varphi_0, \\ \beta &= \frac{1}{R}\frac{d}{d\varphi}\left(2\Omega\sin\varphi\right)_{\varphi_0} = \frac{2\Omega}{R}\cos\varphi_0. \end{aligned}\right\} \tag{1.1.3}$$

This is called the *beta-plane* approximation.

We have denoted the friction force on a fluid particle by $\vec{F}(\vec{v})$ in (1.1.1). It can take various forms depending on the flow conditions. For laminar flow of an incompressible Newtonian fluid it becomes

$$\vec{F} = \upsilon\left(\frac{\partial^2}{\partial x^2} + \frac{\partial^2}{\partial y^2} + \frac{\partial^2}{\partial z^2}\right)\vec{v} \equiv \upsilon\nabla^2\vec{v}, \tag{1.1.4}$$

where υ is the *molecular* viscosity, and $\nabla^2 \equiv \partial^2/\partial x^2 + \partial^2/\partial y^2 + \partial^2/\partial z^2$ is the Laplace operator. In cases when a large scale mean motion occurs in a turbulent environment, we may take

$$\vec{F} = \nabla_A^2\vec{v}, \tag{1.1.5}$$

where $\nabla_A^2 \equiv A^{(x)}\frac{\partial^2}{\partial x^2} + A^{(y)}\frac{\partial^2}{\partial y^2} + A^{(z)}\frac{\partial^2}{\partial z^2}$. Here $A^{(x)}$, $A^{(y)}$, $A^{(z)}$ are the *turbulent* eddy viscosity coefficients in the x-, y-, and z-directions respectively (or for short; *eddy*

viscosities). The eddy viscosities $A^{(x)}$, $A^{(y)}$ and $A^{(z)}$ are generally different, but they are all much larger than the *molecular* viscosity. Usually we have

$$A^{(x)} \sim A^{(y)} > A^{(z)} >> \upsilon \quad . \tag{1.1.6}$$

The eddy viscosities can vary in time and space, but we here assume that they are constants. In some cases where it is important to introduce frictional damping without complicated mathematics, we may take

$$\vec{F} = -r\vec{v}\,, \tag{1.1.7}$$

where *r* is a constant friction coefficient. This last version is called Rayleigh friction, and is formally similar to frictional damping in a porous medium (Darcy friction). Finally, in applications where one studies the vertically integrated fluid properties, the horizontal friction force components are often expressed in terms of the horizontal frictional shear stresses $\tau^{(x)}, \tau^{(y)}$ as

$$F^{(x)} = \frac{\partial}{\partial z}\left(\frac{\tau^{(x)}}{\rho}\right), \quad F^{(y)} = \frac{\partial}{\partial z}\left(\frac{\tau^{(y)}}{\rho}\right), \tag{1.1.8}$$

The conservation of mass for a fluid particle can be expressed mathematically as

$$\nabla \cdot \vec{v} = -\frac{1}{\rho}\left(\frac{\partial \rho}{\partial t} + \vec{v} \cdot \nabla \rho\right) \equiv -\frac{1}{\rho}\frac{D\rho}{dt} \tag{1.1.9}$$

As long as we do not consider sound waves, we can neglect the small variation of density following a fluid particle. The conservation of mass then reduces to

$$\nabla \cdot \vec{v} = 0\,. \tag{1.1.10}$$

This relation (the continuity equation) actually expresses the conservation of volume. It is of course exact for a fluid of constant density (homogeneous incompressible fluid). However, we shall use (1.1.10) throughout this text for all oceanic applications.

Since the free surface is a material surface, the kinematic boundary condition can be written as

$$\frac{D}{dt}(z-\eta)=0,\ \ z=\eta(x,y,t)\,, \tag{1.1.11}$$

or, equivalently

$$w=\frac{D\eta}{dt},\quad z=\eta\,. \tag{1.1.12}$$

The kinematic boundary condition at the bottom becomes

$$\frac{D}{dt}(z+H)=0,\ \ z=-H(x,y)\,, \tag{1.1.13}$$

or

$$w=-\vec{v}\cdot\nabla H\quad z=-H\,. \tag{1.1.14}$$

1.2 Equations for the Lagrangian volume transport

By integrating the continuity equation $\nabla\cdot\vec{v}=0$ in the vertical, and applying the boundary conditions (1.1.12) and (1.1.14), we find exactly

$$\eta_t=-\frac{\partial}{\partial x}\int_{-H}^{\eta}u\,dz-\frac{\partial}{\partial y}\int_{-H}^{\eta}v\,dz\,, \tag{1.2.1}$$

where a subscript denotes partial differentiation. Throughout this text we will alternate between writing partial derivatives in full, and (for economic reasons) as subscripts. The integrals in (1.2.1) are volume transports per unit length in the *x*- and *y*-direction, respectively. Since we here integrate between material surfaces (the bottom and the free surface) theses fluxes are the *Lagrangian* volume fluxes:

$$\left.\begin{aligned}U_L&=\int_{-H}^{\eta}u\,dz,\\ V_L&=\int_{-H}^{\eta}v\,dz.\end{aligned}\right\} \tag{1.2.2}$$

This means that (1.2.2) captures the total flux of fluid particles through vertical planes. Hence, (1.2.1) becomes

$$\eta_t=-U_{Lx}-V_{Ly}\,. \tag{1.2.3}$$

In the momentum equations (1.1.1) we apply the Boussinesq approximation, i.e. we assume that the density changes are only important in connection with the action of gravity. This means that we can take $\rho = \rho_r$, where ρ_r is a constant reference density, in the horizontal components of (1.1.1). Integrating the acceleration term in (1.1.1), using the boundary conditions, we find exactly

$$\begin{aligned} \int_{-H}^{\eta}(u_t + \vec{v}\cdot\nabla u)dz &= U_{Lt} + \frac{\partial}{\partial x}\int_{-H}^{\eta} u^2 dz + \frac{\partial}{\partial y}\int_{-H}^{\eta} vu\,dz, \\ \int_{-H}^{\eta}(v_t + \vec{v}\cdot\nabla v)dz &= V_{Lt} + \frac{\partial}{\partial x}\int_{-H}^{\eta} uv dz + \frac{\partial}{\partial y}\int_{-H}^{\eta} v^2\, dz. \end{aligned} \quad . \qquad (1.2.4)$$

Assuming that $p = P_S(x,y,t),\ z = \eta$, we obtain from the horizontal pressure terms in (1.1.1)

$$\begin{aligned} -\frac{1}{\rho_r}\int_{-H}^{\eta} p_x dz &= -\frac{1}{\rho_r}\left(\frac{\partial}{\partial x}\int_{-H}^{\eta} p dz - P_S\eta_x - P_B H_x\right), \\ -\frac{1}{\rho_r}\int_{-H}^{\eta} p_y dz &= -\frac{1}{\rho_r}\left(\frac{\partial}{\partial y}\int_{-H}^{\eta} p dz - P_S\eta_y - P_B H_y\right), \end{aligned} \qquad (1.2.5)$$

where we have defined the bottom pressure $P_B = p(-H)$. We then may write for the horizontal fluxes

$$\begin{aligned} U_{Lt} - fV_L &= -\frac{1}{\rho_r}\frac{\partial}{\partial x}\int_{-H}^{\eta} p dz + \frac{P_S}{\rho_r}\eta_x + \frac{P_B}{\rho_r}H_x + \int_{-H}^{\eta} F^{(x)}dz - \frac{\partial}{\partial x}\int_{-H}^{\eta} u^2 dz - \frac{\partial}{\partial y}\int_{-H}^{\eta} vu dz, \\ V_{Lt} + fU_L &= -\frac{1}{\rho_r}\frac{\partial}{\partial y}\int_{-H}^{\eta} p dz + \frac{P_S}{\rho_r}\eta_y + \frac{P_B}{\rho_r}H_y + \int_{-H}^{\eta} F^{(y)}dz - \frac{\partial}{\partial x}\int_{-H}^{\eta} uv dz - \frac{\partial}{\partial y}\int_{-H}^{\eta} v^2 dz. \end{aligned} \qquad (1.2.6)$$

In later applications we shall simplify these exact equations (exact under the Boussinesq approximation), and find them very useful.

1.3 Shallow water dynamics

If the horizontal length scale of the motion is very much larger than the vertical length scale (which never can be larger than the ocean depth), the main balance in the vertical momentum equation (1.1.1) is hydrostatic, i.e.

$$p_z = -\rho g \,. \tag{1.3.1}$$

This is the basis for what we denote as *shallow-water* dynamics. It means, when we return to the vertical component in (1.1.1), that the vertical acceleration *Dw*/*dt* and the friction force must be so small that they do not noticeably alter the hydrostatic pressure distribution. A more quantitative discussion of this problem is found in Sec. 2.4. In this case we can write the pressure

$$p = g\int_z^\eta \rho(x,y,z',t)dz' + P_S(x,y,t)\,. \tag{1.3.2}$$

For a homogeneous ocean, the density is constant $(=\rho_0)$. Then

$$p = -\rho_0 g(z-\eta) + P_S\,. \tag{1.3.3}$$

If we disregard the effect of friction for this case, the horizontal components of (1.1.1) can thus be written

$$\frac{Du}{dt} - fv = -g\eta_x - \frac{1}{\rho_0}P_{Sx} \tag{1.3.4}$$

$$\frac{Dv}{dt} + fu = -g\eta_y - \frac{1}{\rho_0}P_{Sy} \tag{1.3.5}$$

We realize that the right-hand sides of (1.3.4) and (1.3.5) are independent of *z*. By utilizing that $v \equiv Dy/dt$ and $f = f_0 + \beta y$, (1.3.4) can be written

$$\frac{D}{dt}\left(u - f_0 y - \frac{1}{2}\beta y^2\right) = -g\eta_x - \frac{1}{\rho_0}P_{Sx} \tag{1.3.6}$$

From (1.3.6) it follows that $D(u - f_0 y - \beta y^2/2)/dt$ is independent of *z*. Thus, this is also true for $(u - f_0 y - \beta y^2/2)$, and thereby also for *u*, if *u* and *v* were independent of

z at time $t = 0$. Similarly, from (1.3.5) we find that v is independent of z. We can accordingly write

$$\left.\begin{aligned} u &= u(x,y,t), \\ v &= v(x,y,t). \end{aligned}\right\} \tag{1.3.7}$$

Furthermore, it now follows from (1.1.10) that w_z is independent of z. Hence, by integrating in the vertical:

$$w = -(u_x + v_y)z + C(x,y,t)\,. \tag{1.3.8}$$

The function C is obtained by applying the boundary condition (1.1.14) at the ocean bottom. The vertical velocity can thus be written

$$w = -(u_x + v_y)(z + H) - uH_x - vH_y\,. \tag{1.3.9}$$

Since u and v here are independent of z, (1.3.4) and (1.3.5) reduce to

$$u_t + uu_x + vu_y - fv = -g\eta_x - \frac{1}{\rho}P_{Sx}\,, \tag{1.3.10}$$

$$v_t + uv_x + vv_y + fu = -g\eta_y - \frac{1}{\rho}P_{Sy}\,, \tag{1.3.11}$$

From (1.2.3) we easily obtain

$$\eta_t + \big(u(H+\eta)\big)_x + \big(v(H+\eta)\big)_y = 0\,. \tag{1.3.12}$$

To solve this set of equations we require three initial conditions, e.g. the distribution of u, v, and η in space at time $t = 0$. If the fluid is limited by lateral boundaries (walls), we must in addition ensure that the solutions satisfy the requirements of no flow through impermeable walls. We repeat that the validity of (1.3.10)-(1.3.12) rest on (i): hydrostatic balance in the vertical direction (shallow-water assumption), (ii): constant density, and (iii): no friction.

1.4 Conservation of potential vorticity

We return to the inviscid, homogeneous, shallow-water ocean. For this case we may derive a very powerful theorem governing the potential vorticity. First, we define the vertical component of the *relative* vorticity in our coordinate system by

$$\zeta = v_x - u_y \,. \tag{1.4.1}$$

In addition, every particle in this coordinate system possesses a *planetary* vorticity *f*, arising from solid body rotation with angular velocity $\Omega \sin\varphi$. Hence, the *absolute* vertical vorticity for a particle becomes $f + \zeta$. We shall derive an equation for the absolute vorticity. It is obtained by differentiating the equations (1.3.10) and (1.3.11) by $-\partial/\partial y$ and $\partial/\partial x$, respectively, and then add the resulting equations. Mathematically, this means to operate the curl on the vector equation to eliminate the gradient terms. Since *f* is independent of time, we find that

$$\frac{D}{dt}(f + \zeta) = -(f + \zeta)(u_x + v_y) \,. \tag{1.4.2}$$

By using that *H* is independent of time (1.3.12) can be written

$$\frac{D}{dt}(H + \eta) = -(H + \eta)(u_x + v_y) \,. \tag{1.4.3}$$

Here, $H + \eta$ is the height of a vertical fluid column. We define the *potential vorticity* *Q* by

$$Q \equiv \frac{f + \zeta}{H + \eta} \,. \tag{1.4.4}$$

By eliminating the horizontal divergence between (1.4.2) and (1.4.3), we find for *Q* that

$$\frac{DQ}{dt} = 0 \,. \tag{1.4.5}$$

This equation expresses the fact that a given material vertical fluid column always moves in such a way that its potential vorticity is conserved.

Alternatively, we can apply Kelvin's circulation theorem for an inviscid fluid to derive this important result. Kelvin's theorem states that the circulation of the absolute velocity around a closed material curve (always consisting of the same fluid particles) is conserved. For a material curve Γ in the horizontal plane, Kelvin's and Stokes' theorems yield

$$\oint_{\Gamma} \vec{v}_{abs} \cdot \delta\vec{r} = \iint_{\sigma} \vec{k} \cdot (\nabla \times \vec{v}_{abs}) \delta\sigma = \text{const.}, \tag{1.4.6}$$

where σ is the area inside Γ. Furthermore, in the surface integral:

$$\vec{k} \cdot (\nabla \times \vec{v}_{abs}) = f + \zeta\,. \tag{1.4.7}$$

When the surface area σ in (1.4.6) approaches zero, we have

$$(f + \zeta)\delta\sigma = \text{const.} \tag{1.4.8}$$

In addition, the mass of a vertical fluid column with base $\delta\sigma$ must be conserved, and hence

$$\rho(H + \eta)\delta\sigma = \text{const.} \tag{1.4.9}$$

This is valid for all times, since a vertical fluid column will remain vertical; see (1.3.7). In our case the fluid is homogeneous and incompressible, i.e. ρ is the same for all particles. Thus, by eliminating $\delta\sigma$ between (1.4.8) and (1.4.9), we find as before that

$$Q = \frac{f + \zeta}{H + \eta} = \text{const.}, \tag{1.4.10}$$

or, equivalently, $DQ/dt = 0$.

In the ocean we usually have that $|\zeta| << f$ and $|\eta| << H$. For stationary flow, assuming that $|\nabla H| >> |\nabla \eta|$ and $|f \nabla H| >> |H \nabla \zeta|$, (1.4.5) yields approximately that

$$\vec{v} \cdot \nabla(f / H) = 0\,. \tag{1.4.11}$$

On an *f*-plane, this equation reduces to

$$\vec{v} \cdot \nabla H = 0 . \tag{1.4.12}$$

Accordingly, the flow in this case follows the lines of constant H (i.e. the bottom contours). This phenomenon is called *topographic steering*. On a beta-plane the flow will follow the contours of the function f / H (the geostrophic contours); see (1.4.11).

1.5 The storm surge equations

From experience we know that when it comes to computing the change of sea level due to atmospheric wind and pressure fields, we can apply the hydrostatic approximation (1.3.2), and neglect the density variation in the vertical. For such motion, referred to as *storm surge*, the water appears to be quasi-homogeneous, and we can use a constant reference density everywhere. Furthermore, the horizontal velocities are fairly small, which can justify the neglect of the nonlinear convective acceleration terms on the right-hand side of (1.2.6). This linearization is also consistent with the assumption that $|\eta| << H$. The volume fluxes in this linear problem are the Eulerian fluxes given by

$$U_E = \int_{-H}^{0} u dz, \quad V_E = \int_{-H}^{0} v dz . \tag{1.5.1}$$

Utilizing a friction force of the type (1.1.8), we then find for the storm surge problem:

$$\begin{aligned} U_{Et} - fV_E &= -gH\eta_x - HP_{Sx} / \rho_r + \tau_S^{(x)} / \rho_r - \tau_B^{(x)} / \rho_r , \\ V_{Et} + fU_E &= -gH\eta_y - HP_{Sy} / \rho_r + \frac{1}{\rho_r}\tau_S^{(y)} - \frac{1}{\rho_r}\tau_B^{(y)} , \\ \eta_t &= -\left(U_{Ex} + V_{Ey}\right). \end{aligned} \tag{1.5.2}$$

Here $(\tau_S^{(x)}, \tau_S^{(y)})$ are the wind stresses along the mean position of the ocean surface $z = 0$, and $(\tau_B^{(x)}, \tau_B^{(y)})$ are the frictional stresses at the bottom $z = -H(x, y)$. For operational use, the surface pressure gradients are obtained from weather

analyses/prognoses, and the wind stresses are usually related to the wind speed (u_{10}, v_{10}) at 10 m height through

$$\vec{\tau}_S = \rho_a c_D |\vec{v}_{10}| \vec{v}_{10} . \qquad (1.5.3)$$

Here ρ_a is the density of air, and c_D is a drag coefficient which is typically in the range $1\times10^{-3} - 3\times10^{-3}$ (higher values for stronger winds). The bottom friction is more difficult to model. Sometimes a linear friction in the fluxes is applied, i.e.

$$\vec{\tau}_B = \rho_r K \vec{V}_E , \qquad (1.5.4)$$

where *K* is a constant bottom friction coefficient. More frequently, friction laws that are quadratic in the mean velocity are used at the bottom.

It is important to realize that (1.5.2) is a linearized set of equations for the Eulerian volume fluxes (1.5.1). Unlike the nonlinear Lagrangian fluxes (1.2.2), they do not contain any mean wave momentum. Hence the storm surge equations only yield the surface elevation and mean currents induced by wind stress and atmospheric pressure gradients along the sea surface. In Chapter V we return to the intriguing problem of mean currents induced by surface waves in the ocean.

II. ADJUSTMENT UNDER GRAVITY IN A HOMOGENEOUS, NON-ROTATING OCEAN

2.1 Linear waves in an ocean of finite depth

For a homogeneous fluid at rest, the surface is horizontal. If we initially establish a surface elevation which deviates from the horizontal, the subsequent motion will be in the form of surface gravity waves. Since the density of the ocean is about one thousand times larger than the density of the atmosphere, we can neglect the effect of the air on the oceanic wave motion. In this chapter we consider surface gravity waves

with short periods much shorter than the inertial period $2\pi / f$ (~16 hrs at mid latitude). It is obvious that the earth's rotation will have very little effect on the orbital motion in such waves, so we can neglect it. For the moment we also neglect the effect of friction on the wave motion. This is motivated by the fact that wind-generated waves in the open ocean (swell) may propagate for hundreds of kilometres without being severely damped[1]. From (1.1.1) the momentum equation now reduces to

$$\frac{D\vec{v}}{dt} = -\frac{1}{\rho_0}\nabla p - g\vec{k}\,, \tag{2.1.1}$$

where ρ_0 is the constant density. For this case we have from Kelvin's theorem for the velocity circulation along a material closed curve γ:

$$\frac{d}{dt}\oint_{\gamma}\vec{v}\cdot d\vec{r} = 0\,. \tag{2.1.2}$$

If the velocity circulation initially is zero, which we here assume, it will remain zero for all times, i.e.

$$\int_{\gamma}\vec{v}\cdot d\vec{r} = 0\,. \tag{2.1.3}$$

Then the velocity can be derived from a potential ϕ, i.e.

$$\vec{v} = \nabla\phi\,, \tag{2.1.4}$$

or

$$u = \phi_x,\ v = \phi_y,\ w = \phi_z\,. \tag{2.1.5}$$

Accordingly, from the continuity equation $\nabla\cdot\vec{v} = 0$ we obtain

$$\nabla^2\phi = 0\,. \tag{2.1.6}$$

In general we have that

[1] However, we will see later on that the effect of friction as well as the Coriolis force will be important for determining the nonlinear mean current (the drift) induced by surface waves.

$$\nabla\left(\frac{1}{2}\vec{v}^2\right) = \vec{v}\cdot\nabla\vec{v} + \vec{v}\times(\nabla\times\vec{v})\,. \tag{2.1.7}$$

Since the last term here (the vorticity) is zero from (2.1.4), we realize that (2.1.1) can be written

$$\nabla\left(\frac{p}{\rho_0} + \phi_t + \frac{1}{2}(\nabla\phi)^2 + gz\right) = 0\,. \tag{2.1.8}$$

When integrating this equation in space, the integration constant can be set equal to zero. Hence

$$\frac{p}{\rho_0} = -\phi_t - \frac{1}{2}(\nabla\phi)^2 - g\,z\,. \tag{2.1.9}$$

This is the Euler equation for the pressure.

If the ocean bed is flat, which we assume here, and situated at $z = -H$, we must have at the ocean bottom

$$w = \frac{\partial\phi}{\partial z} = 0, \quad z = -H. \tag{2.1.10}$$

This constitutes the kinematic boundary condition at the ocean bottom.

In this chapter we consider waves with *small* amplitudes. As a first approximation we neglect terms in the governing equations that are proportional to the square of the wave amplitude, i.e. we *linearize* our equations. In this approximation, the kinematic boundary condition at the surface becomes

$$\frac{\partial\eta}{\partial t} = w = \frac{\partial\phi}{\partial z}, \quad z = 0\,, \tag{2.1.11}$$

We consider a wave solution in the form of a complex Fourier component

$$\eta = A\exp(i(kx - \omega t))\,. \tag{2.1.12}$$

From (2.1.6), (2.1.10), and (2.1.11) we then obtain

$$\phi = -\frac{i\omega A\cosh(k(z+H))}{k\sinh(kH)}\exp i(kx - \omega t)\,. \tag{2.1.13}$$

Hence, the real parts of the velocities in the ocean can be written

$$u = \frac{\omega A \cosh(k(z+H))}{\sinh(kH)} \cos(kx - \omega t),$$
$$w = \frac{\omega A \sinh(k(z+H))}{\sinh(kH)} \sin(kx - \omega t). \tag{2.1.14}$$

For the real part of the pressure we find from the linearized version of (2.1.9) that

$$\frac{p}{\rho_0} = \frac{\omega^2 A \cosh(k(z+H))}{k \sinh(kH)} \cos(kx - \omega t) - gz\,. \tag{2.1.15}$$

For surface waves in the ocean we can neglect the effect of the air above the water. This means that we can take $p = 0$ at the surface. Hence, from the dynamic boundary condition $p(\eta) = 0$, the linearized version of (2.1.9) yields

$$\eta = A\cos(kx - \omega t) = \frac{\omega^2 A \cosh(k(\eta + H))}{gk \sinh(kH)} \cos(kx - \omega t)\,. \tag{2.1.16}$$

Utilizing that $|\eta| << H$, we obtain for the frequency

$$\omega^2 = gk \tanh(kH)\,. \tag{2.1.17}$$

For waves propagating in the positive *x*-direction, we find for the phase speed that

$$c = \frac{\omega}{k} = \left(\frac{g\lambda \tanh(2\pi H/\lambda)}{2\pi} \right)^{1/2}. \tag{2.1.18}$$

It is readily seen that *c* increases monotonically with increasing wavelength. Such waves are called dispersive waves (positive dispersion). Hence, for an ensemble of waves with various wavelengths generated at a certain location, the longer waves will move faster, and disappear from the generation area. This is like ocean swell escaping from the storm centre. The extreme cases of (2.1.18) are (a): Deep-water waves ($kH >> 1$). Then

$$c = \frac{\omega}{k} = \left(\frac{g\lambda}{2\pi} \right)^{1/2}. \tag{2.1.19}$$

(b): Waves in shallow water ($kH << 1$). Then

$$c = (gH)^{1/2}. \tag{2.1.20}$$

To first order in wave amplitude we find that individual fluid particles in surface wave motion moves in closed paths. If the Lagrangian coordinates of a single particle is (x_L, z_L), we can write

$$\frac{\partial x_L}{\partial t} = u, \quad \frac{\partial z_L}{\partial t} = w, \tag{2.1.21}$$

where *u* and *w* are given by (2.1.14). Defining

$$R_1 = \frac{A\cosh(k(z+H))}{\sinh(kH)}, \quad R_2 = \frac{A\sinh(k(z+H))}{\sinh(kH)}, \tag{2.1.22}$$

we find from (2.1.21) that

$$\frac{(x_L - x_0)^2}{R_1^2} + \frac{(z_L - z_0)^2}{R_2^2} = 1. \tag{2.1.23}$$

We realize that the particle path is elliptic with centre in (x_0, z_0). The major half axis is R_1, and the minor half axis is R_2. They both decrease with depth. For infinitely deep water, $R_1 \to R_2$, and the particles move in circles. We shall see in Chapter V that when we consider nonlinear wave motion, the particle path is not closed. Each particle has a forward spiralling motion which gives rise to a mean forward drift of particles. This means that waves do induce a current in the medium through which they propagate.

2.2 Wave groups and group velocity

Up to now we have considered one single wave component. If we have two wave components the same amplitude, but with slightly different wave numbers and frequencies, they can be written in complex form as

$$\eta_+ = \frac{1}{2} A \exp i\{(k+\Delta k)x - (\omega+\Delta\omega)t\},$$
$$\eta_- = \frac{1}{2} A \exp i\{(k-\Delta k)x - (\omega-\Delta\omega)t\}, \tag{2.2.1}$$

where $|\Delta k/k| << 1, \quad |\Delta\omega/\omega| << 1$. Each of the two components above is a solution to our wave problem. Since we work with linear theory, also the sum $\eta_+ + \eta_-$ of the two components becomes a solution. This superposition can be written

$$\begin{aligned}\eta_+ + \eta_- &= \frac{1}{2} A \exp i(kx-\omega t)\left[\exp i(\Delta kx - \Delta\omega t) + \exp(-i(\Delta kx - \Delta\omega t))\right] \\ &= A\cos\Delta k\left(x - \frac{\Delta\omega}{\Delta k}t\right)\exp i(kx-\omega t).\end{aligned} \tag{2.2.2}$$

We denote the real part of (2.2.2) by η, representing the physical solution. We then find

$$\eta = A\cos\left(\Delta k\left(x - \frac{\Delta\omega}{\Delta k}t\right)\right)\cos\left(k\left(x - \frac{\omega}{k}t\right)\right). \tag{2.2.3}$$

This shows that η is an amplitude-modulated wave train consisting of series of wave groups, as shown in Fig. 2.1, where we have plotted η/A as a function of *x* for $\Delta k/k = 0.1$.

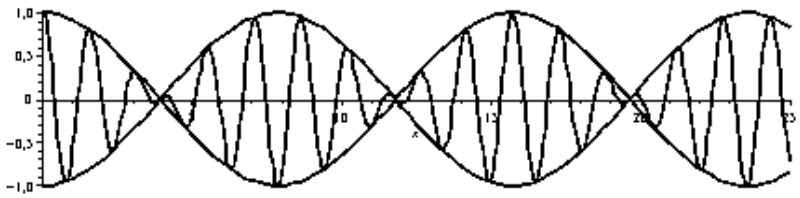

Fig. 2.1 *Sketch of wave groups.*

The individual waves in the group will propagate with the ordinary phase speed $c = \omega/k$, while the group itself will propagate with the group velocity $c_g = \Delta\omega/\Delta k$.

In the limit when $\Delta k \to 0$, the group velocity becomes the derivative of the frequency with respect to the wave number, i.e.

$$c_g = \frac{d\omega}{dk}. \tag{2.2.4}$$

Since $\omega = kc$, and $k = 2\pi/\lambda$, we note that (2.2.4) can be written as

$$c_g = c - \lambda \frac{dc}{d\lambda}. \tag{2.2.5}$$

So, if the phase speed increases with increasing wavelength (normal dispersion), then $c_g < c$. If the phase speed is independent of the wavelength (non-dispersive waves), we have that $c_g = c$.

It is a simple exercise to show from (2.1.17) and (2.2.4) that the general relation between the group velocity and the phase velocity for surface waves becomes

$$\frac{c_g}{c} = \frac{1}{2}\left(1 + \frac{2kH}{\sinh(2kH)}\right). \tag{2.2.6}$$

2.3 The motion of a pulse in a shallow channel

In the previous analysis we have used the concept of Fourier components to describe the wave form. However for shallow-water waves, which are non-dispersive, we can easily derive solutions for arbitrary surface displacements. We assume small disturbances from the state of equilibrium in the ocean, two-dimensional motion ($\partial/\partial y = 0$, $v = 0$), and constant depth. For linearized, shallow-water waves in the x-direction (2.1.1) reduces to

$$\left.\begin{aligned} u_t &= -g\eta_x, \\ \eta_t &= -Hu_x. \end{aligned}\right\} \tag{2.3.1}$$

Eliminating the horizontal velocity, we find

$$\eta_{tt} - gH\eta_{xx} = 0. \tag{2.3.2}$$

This equation is called the *wave equation*, and appears in many places in physics. Instead of assuming a single Fourier component as solution of this equation, we realize immediately that a general solution can be written

$$\eta = F_1(x + c_0 t) + F_2(x - c_0 t), \tag{2.3.3}$$

where $c_0 = (gH)^{1/2}$. If, at time $t = 0$, the surface elevation was such that $\eta = F(x)$, and $\eta_t = 0$, it is easy to see that the solution becomes

$$\eta = \frac{1}{2}\{F(x + c_0 t) + F(x - c_0 t)\}. \tag{2.3.4}$$

From (2.3.1) and (2.3.3) we find for the acceleration

$$u_t = -g\eta_x = -\frac{g}{2}\{F'(x + c_0 t) + F'(x - c_0 t)\}, \tag{2.3.5}$$

where $F'(\xi) = dF/d\xi$. Hence, the horizontal velocity is given by

$$u = -\frac{g}{2c_0}\{F(x + c_0 t) - F(x - c_0 t)\}. \tag{2.3.6}$$

From (2.3.4) we can display the evolution of an initially bell-shaped surface elevation $F(x)$ with typical width L; see the sketch in Fig. 2.2.

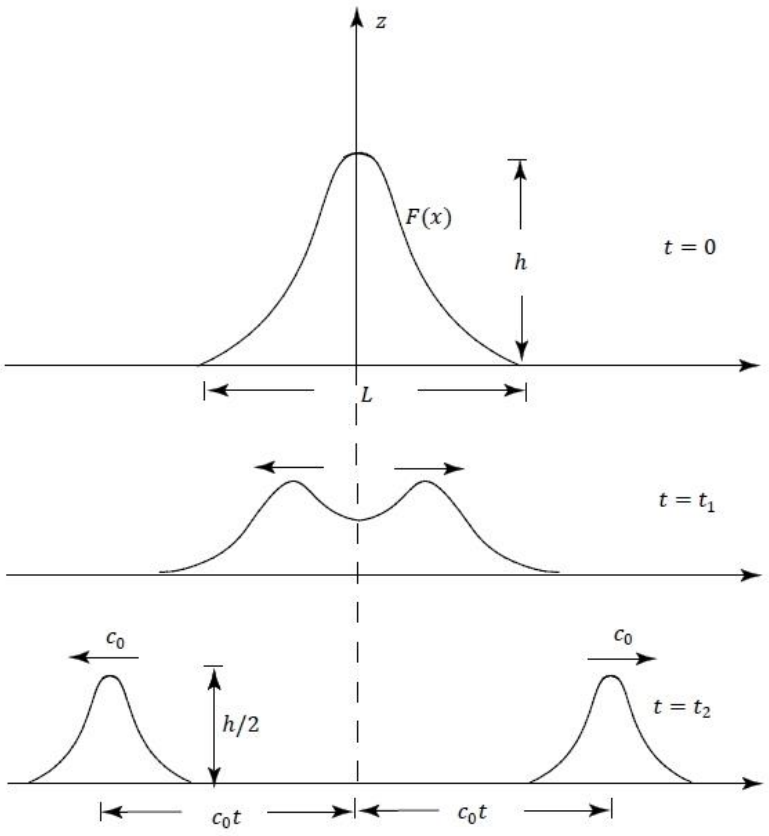

Fig. 2.2 *Evolution of a bell-shaped surface elevation.*

We note that the initial elevation splits into two identical pulses moving right and left with velocity $c_0 = (gH)^{1/2}$. In a deep ocean (H = 4000 m), the phase speed is $c_0 \approx 200$ m s^{-1}, while in a shallow ocean (H = 100 m) we have $c_0 \approx 30$ m s^{-1}. If the maximum initial elevation in this example is h, i.e. $F(0) = h$, we find from (2.3.6) that the velocity in the ocean directly below peak of the right-hand pulse can be written

$$u = \frac{gh}{2c_0}, \tag{2.3.7}$$

when $t >> L/c_0$, that is after the two pulses have split. If we take h = 1 m as a typical value, the deep ocean example yields $u \approx 2.5$ cm s^{-1}, while for the shallow ocean we find $u \approx 17$ cm s^{-1}.

As a second example we consider an initial step function:

$$F(x)=\begin{cases} \frac{1}{2}h, & x>0, \\ -\frac{1}{2}h, & x<0. \end{cases} \tag{2.3.8}$$

In this case, the velocity and amplitude development becomes as sketched in Fig. 2.3.

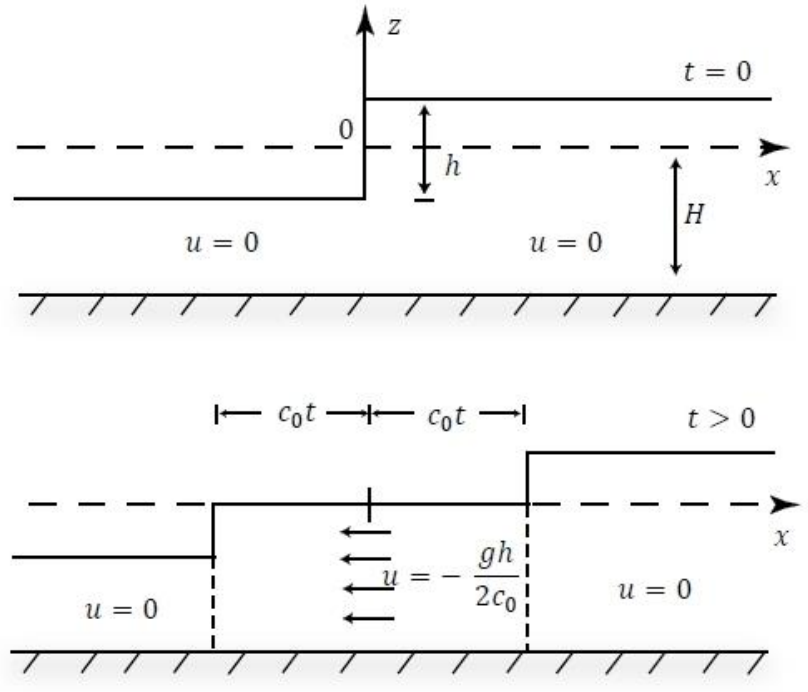

Fig. 2.3 *Evolution of a surface step function*.

It is obvious that we in an example like this (with a step in the surface at $t = 0$) must be careful when using linear theory, which requires small gradients. In a more realistic example where differences in height occurs, the initial elevation will have a final (an quite small) gradient around $x = 0$. Qualitatively, however, the solution becomes as discussed above.

2.4 Validity of the hydrostatic approximation

Let us consider the validity of the hydrostatic approximation in the case of waves in a non-rotating ocean. We rewrite the pressure as a hydrostatic part plus a deviation:

$$p = \rho_0 g(\eta - z) + P_S + p', \tag{2.4.1}$$

where p' is the non-hydrostatic deviation. The vertical component of (2.1.1) becomes to lowest order:

$$w_t = -\frac{1}{\rho_0} p'_z, \tag{2.4.2}$$

while the horizontal component can be written

$$u_t = -g\eta_x - \frac{1}{\rho_0} p'_x. \tag{2.4.3}$$

The hydrostatic assumption implies that

$$\left| \frac{1}{\rho_0} p'_x \right| << |u_t|. \tag{2.4.4}$$

If the typical length scales in the x- and z-directions are L and H, respectively, we obtain from the continuity equation that

$$|u| \sim \frac{L}{H} |w|, \tag{2.4.5}$$

where ~ means order of magnitude. From (2.4.2) we then find

$$\left| \frac{p'}{\rho} \right| \sim \frac{H^2}{L} |u_t|. \tag{2.4.6}$$

Utilizing this result, the condition (2.4.4) reduces to

$$H^2 / L^2 << 1. \tag{2.4.7}$$

Thus, we realize that the assumption of a hydrostatic pressure distribution in the vertical requires that the horizontal scale L of the disturbance must be much larger than the ocean depth. For a wave, L is associated with the wavelength; for a single pulse, L corresponds to the characteristic pulse width.

2.5 Energy transport in surface waves

As mentioned in Section 2.1, a local wind event in the open deep ocean generates wind waves with many different wavelengths. Since such waves are dispersive, the longest waves will travel fastest. For example, for a wavelength of 300 m, we find that the phase speed is nearly 22 m/s. These waves may propagate faster than the low pressure system that generated then, and hence escape from the storm region. Such waves are called *swell*, and may propagate for hundreds of kilometres through the ocean till they finally reach the coast, gradually transforming to shallow-water waves. Finally, they break in the surf zone on the beach, and loose their mechanical energy. In this way we understand that waves are carriers of energy. They get their energy from the wind, propagate the energy over large distances, and loose it by doing work on the beaches in the form of beach erosion processes etc. If there is any rest mechanical energy, it is transferred to heat in the breaking process.

The total mechanical energy E per unit area in surface waves is the sum of the mean kinetic energy E_k and the mean potential energy E_p. Per definition

$$E_k = \frac{1}{T}\int_0^T \left(\frac{1}{2}\rho_0 \int_{-H}^{\eta} (u^2 + w^2) dz \right) dt \approx \frac{1}{T}\int_0^T \left(\frac{1}{2}\rho_0 \int_{-H}^{0} (u^2 + w^2) dz \right) dt \,, \qquad (2.5.1)$$

where $T = 2\pi/\omega$ is the wave period. For periodic wave motion we assume that the potential energy is zero at the mean surface level. Hence

$$E_p = \frac{1}{T}\int_0^T \left(\rho_0 g \int_0^{\eta} z dz \right) dt \,. \qquad (2.5.2)$$

Inserting from (2.1.12) and (2.1.14), we obtain after some algebra that

$$E_k = E_p = \frac{1}{4}\rho_0 g A^2 \,. \qquad (2.5.3)$$

Hence, the mechanical energy is equally partitioned between kinetic and potential energy. The total energy per unit area, often referred to as the *energy density*, becomes

$$E = E_k + E_p = \frac{1}{2}\rho_0 g A^2 . \tag{2.5.4}$$

The mean horizontal energy flux F_e is the work per unit time done by the dynamic (fluctuating) pressure in displacing particles horizontally. By definition

$$F_e = \frac{1}{T}\int_0^T \left(\int_{-H}^{\eta} pudz \right) dt \approx \frac{1}{T}\int_0^T \left(\int_{-H}^{0} pudz \right) dt . \tag{2.5.5}$$

Applying the horizontal velocity in (2.1.14) and the dynamic pressure in (2.1.15) (leaving out the static part $\rho_0 gz$), we find

$$F_e = \frac{\rho_0 \omega^3 A^2}{8k^2 \sinh^2 kH}\left(\sinh(2kH) + 2kH\right). \tag{2.5.6}$$

Utilizing the dispersion relation (2.1.17), and the group velocity given by (2.2.6), we can write the mean energy flux (2.5.6) as

$$F_e = c_g E . \tag{2.5.7}$$

In our earlier treatment of the group velocity it was defined from a purely kinematic point of view. We understand from (2.5.7) that the group velocity has a much deeper significance: It is the velocity that the mean energy in the wave motion travels with. Accordingly, to receive a signal that propagates over a distance L in the form of a wave, we must wait a time $t = L/c_g$, before the receiver picks up the signal.

2.6 The Stokes edge wave

Stokes (1846) discovered a surface wave that could exist in an ocean where the bottom was sloping linearly; see the sketch in Fig. 2.4, where the slope angle is β.

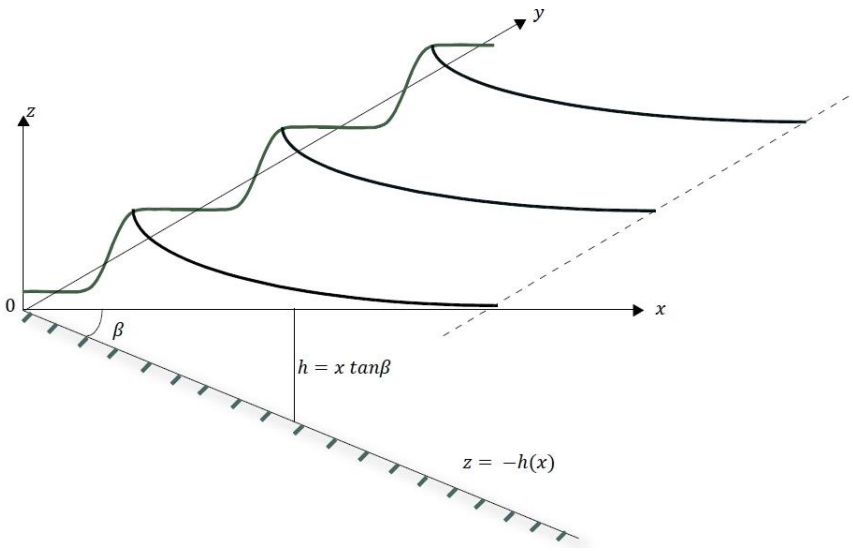

Fig. 2.4 *Sketch of the Stokes edge wave.*

In the absence of viscosity and rotation, the solution can be derived from the Laplace equation (2.1.6). For a wave in the *y*-direction we can write:

$$\phi = F(x,z)e^{i(ky-\omega t)}. \tag{2.6.1}$$

Then Laplace's equation reduces to

$$\frac{\partial^2 F}{\partial x^2} + \frac{\partial^2 F}{\partial z^2} - k^2 F = 0. \tag{2.6.2}$$

We consider exponentially trapped waves in the direction normal to the coast, and assume that the solution decays exponentially with depth, i.e.

$$F = Ce^{-ax+bz}, \quad a,b>0. \tag{2.6.3}$$

Hence, from (2.6.2)

$$a^2 + b^2 - k^2 = 0. \tag{2.6.4}$$

The kinematic boundary condition at the sloping bottom is:

$$w = -\vec{v}\cdot\nabla h, \quad z = -h, \tag{2.6.5}$$

or

$$\phi_z = -(\tan\beta)\phi_x, \quad z = -x\tan\beta. \tag{2.6.6}$$

From (2.6.6) we obtain that $b = a\tan\beta$. Inserting into (2.6.4):

$$a = k\cos\beta, \quad b = k\sin\beta . \tag{2.6.7}$$

Hence, we can write the velocity potential

$$\phi = C\exp\left(-kx\cos\beta + kz\sin\beta + i(ky - \omega t)\right). \tag{2.6.8}$$

From the linearized kinematic boundary at the surface (2.1.11), we find for the surface elevation that

$$\eta = A\exp\left(-kx\cos\beta + i(ky - \omega t)\right). \tag{2.6.9}$$

where $A = iCk\sin\beta/\omega$. The dynamic boundary condition at the surface is $p(z = \eta) = 0$. From the linearized version of (2.1.9) we obtain

$$\phi_t + g\eta = 0, \quad z = 0 . \tag{2.6.10}$$

By inserting into this equation, we find the dispersion relation

$$\omega^2 = gk\sin\beta . \tag{2.6.11}$$

This result is valid for $0 < \beta < \pi/2$. We note that this trapped wave, called the *Stokes edge wave*, can travel along the coast in both directions, due to the two possible signs in (2.6.11).

When the beach slope is small $(\beta << 1)$, we can analyse this problem by using shallow water theory. We then realize that the trapping can be explained by the fact that the local phase speed $\sqrt{gH}$ increases with increasing distance from the coast. If we represent the wave by a ray which is directed along the local direction of energy propagation, e.g. Section 2.8, the ray will always be gradually refracted towards the coast. At the coast, the wave is reflected, and the refraction process starts all over again. The total wave system thus consists of a superposition between an incident and a reflected wave in an area near the coast. The width of this area depends on the angle of incidence with the coast for the ray in question. Outside this region, the wave amplitude decreases exponentially.

When we analyse this problem more thoroughly, we find that the Stokes edge wave is the first mode in a spectrum of shelf modes that contains both discrete and continuous parts; see LeBlond and Mysak (1978), p. 221. If we take the earth's rotation into account ($f \neq 0$), the frequencies for the edge waves in the positive and negative x-directions will be slightly different.

2.7 Wave kinematics

We can generalize the result in this chapter to wave propagation in three dimensions. Let ψ denote the velocity potential or the stream function of a plane wave. By introducing a wave number vector $\vec{\kappa}$ defined by

$$\vec{\kappa} = k_1\vec{i}_1 + k_2\vec{i}_2 + k_3\vec{i}_3, \tag{2.7.1}$$

and a radius vector $\vec{r}$, where

$$\vec{r} = r_1\vec{i}_1 + r_2\vec{i}_2 + r_3\vec{i}_3, \tag{2.7.2}$$

we can write a plane wave as

$$\psi = A\exp(i(\vec{\kappa}\cdot\vec{r} - \omega t)) = A\exp\{i\vec{\kappa}\cdot\left(\vec{r} - \frac{\omega\vec{\kappa}}{\kappa^2}t\right)\}. \tag{2.7.3}$$

The vectorial phase speed $\vec{c}$ is now defined by

$$\vec{c} = \frac{\omega\vec{\kappa}}{\kappa^2}, \qquad \kappa^2 = k_1^2 + k_2^2 + k_3^2. \tag{2.7.4}$$

Furthermore, we can write the components of the vectorial group velocity $\vec{c}_g$ as

$$\left.\begin{aligned} c_g^{(1)} &= \partial\omega/\partial k_1, \\ c_g^{(2)} &= \partial\omega/\partial k_2, \\ c_g^{(3)} &= \partial\omega/\partial k_3. \end{aligned}\right\} \tag{2.7.5}$$

In vector notation this becomes

$$\vec{c}_g = \nabla_\kappa\omega, \quad \nabla_\kappa \equiv \vec{i}_1\frac{\partial}{\partial k_1} + \vec{i}_2\frac{\partial}{\partial k_2} + \vec{i}_3\frac{\partial}{\partial k_3}. \tag{2.7.6}$$

If the frequency ω only is a function of the magnitude of the wave number vector, i.e. $\omega = \omega(\kappa)$, we refer to the system as *isotropic*. If we cannot write the dispersion relation in this way, the system is *anisotropic*. We now consider the surface in wave number space given by $\omega = \omega(k_1, k_2, k_3) = C$, where C is a constant; see Fig. 2.5, where we display a two-dimensional example.

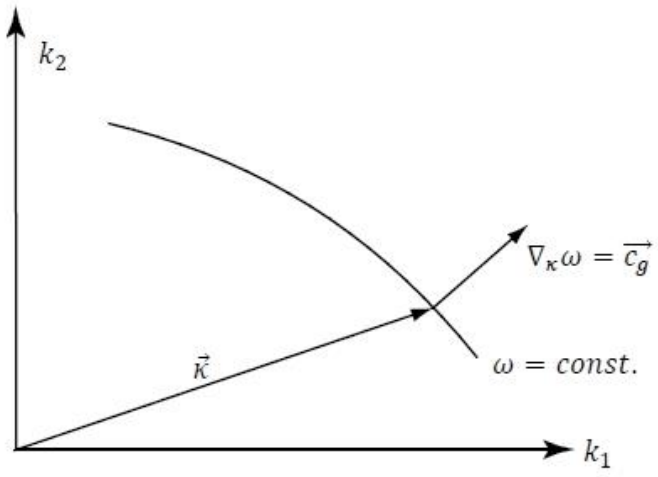

Fig. 2.5 *Constant- frequency surface in wave number space.*

The gradient $\nabla_\kappa \omega$ is always perpendicular to the constant frequency surface. From (2.7.6) we note that this means that the group velocity is always directed along the surface normal, as depicted in Fig. 2.5. Since the phase velocity is directed along the wave number vector, e.g. (2.7.4), we realize that if the phase speed and group velocity should become parallel, then the constant frequency surface must be a sphere in wave number space. Mathematically, this means that $\omega = \omega(\kappa)$, i.e. we have an isotropic system.

2.8 Application to a slowly-varying medium

If the medium through which the waves propagate is not completely spatially uniform or constant in time, the wave train will vary as it propagates. If the length and time scales over which the medium varies are large compared to the wavelength or wave period, the local properties of the wave will vary slowly throughout the field. If ζ represents the displacement of a fluid element, the wave train can be specified by $\zeta = A\exp(i\theta)$, where *A* is the local amplitude, which is a slowly varying function of position and time, and $\theta(\vec{r},t)$ is the phase function. The wave number $\vec{\kappa}$ and the radian frequency ω, which both may be slowly varying functions of space and time, can now be defined as

$$\vec{\kappa} = \nabla\theta, \quad \omega = -\theta_t . \tag{2.8.1}$$

From this it follows that

$$\nabla \times \vec{\kappa} = 0 . \tag{2.8.2}$$

Hence the distribution of the local wave number in space is irrotational. Furthermore, from (2.8.1)

$$\vec{\kappa}_t + \nabla\omega = 0 . \tag{2.8.3}$$

This can be considered as a kinematical conservation equation for the density of waves. In a random field of linearly superposed waves, (2.8.3) holds for each Fourier component. For a steady wave field, $\nabla\omega = 0$. If the waves propagate in the *x*-direction and the dispersion relation have the form $\omega = \omega(k, H(x))$, we have for this case that

$$\frac{d\omega}{dx} = \frac{\partial\omega}{\partial k}\frac{dk}{dx} + \frac{\partial\omega}{\partial H}\frac{dH}{dx} = 0 . \tag{2.8.4}$$

For example, for shallow water waves on a gently sloping beach, we have from (2.1.17) that $\omega = (gH(x))^{1/2}k$. By inserting into (2.8.4), and integrating, we readily find for this case that

$$k(x) = k_0 \left(\frac{H_0}{H(x)} \right)^{1/2}, \tag{2.8.5}$$

where k_0, H_0 are the wave number and the depth at $x = x_0$. We note from (2.8.5) that when the wave propagates into shallower water, like a tsunami approaching the shore, the wave number increases. Accordingly, the wavelength becomes smaller. Together with increasing wave amplitude, this is steepens the wave, which ultimately leads to breaking in the surf zone.

Ray theory

The wave energy propagates in the direction of the group velocity vector. We can define the energy path, or ray, as the curve in to-dimensional space where the tangent at each point is along the group velocity, i.e.

$$d\vec{r} \times \vec{c}_g = 0 . \tag{2.8.6}$$

For example, in the horizontal plane $d\vec{r} = dx\vec{i} + dy\vec{j}$, and hence the equation for the ray becomes

$$\frac{dy}{dx} = \frac{c_g^{(y)}}{c_g^{(x)}} . \tag{2.8.7}$$

If the group velocity components are independent of *x* and *y*, the ray $y = F(x)$ becomes a straight line. However, if we for example consider shallow water waves in an ocean with a slowly varying depth, the group velocity components will vary slowly with the horizontal coordinates. Then the ray will be curved, as mentioned in connection with edge waves in Section 2.6.

Doppler shift

In this analysis the frequency ω is the frequency for waves propagating in a medium at rest. If now the fluid moves with a velocity $\vec{U}$, which can be a slowly varying function of space and time, ω is the frequency that will be found by an observer moving with the undisturbed fluid velocity. It is called the *intrinsic* frequency, and can be obtained from the dispersion relation. However, the frequency *n* measured by an observer at rest, or the *apparent* frequency, will be

$$n = \omega + \vec{\kappa} \cdot \vec{U} . \tag{2.8.8}$$

When the wave and the medium move in the same direction, the last term is positive, and the frequency appears to increase (higher tone) for a fixed observer, while it decreases (lower tone) when they move in opposite directions. This phenomenon is known as *Doppler shift*.

III. SHALLOW-WATER IN WAVES IN A ROTATING, NON-STRATIFIED OCEAN

3.1 The Klein-Gordon equation

We now consider the effect of the earth's rotation upon wave motion in shallow water. Linear theory still applies, and we take the depth and the surface pressure to be constant. Furthermore, we assume that *f* is constant. Equations (1.3.10)-(1.3.12) then reduce to

$$u_t - fv = -g\eta_x , \tag{3.1.1}$$

$$v_t + fu = -g\eta_y , \tag{3.1.2}$$

$$\eta_t + H(u_x + v_y) = 0 . \tag{3.1.3}$$

We compute the vertical vorticity and the horizontal divergence, respectively, from (3.1.1) and (3.1.2). By utilizing (3.1.3), we then obtain

$$(v_x - u_y)_t - \frac{f}{H}\eta_t = 0\,, \tag{3.1.4}$$

and

$$\frac{\eta_{tt}}{H} + f(v_x - u_y) = g(\eta_{xx} + \eta_{yy})\,. \tag{3.1.5}$$

The vorticity equation can be integrated in time, i.e.

$$v_x - u_y - \frac{f}{H}\eta = v_{0x} - u_{0y} - \frac{f}{H}\eta_0\,, \tag{3.1.6}$$

where sub-zeroes denote initial values. We assume that the problem is started from rest, which means that there are no velocities or velocity gradients at $t = 0$. Thus

$$v_x - u_y = -\frac{f}{H}(\eta_0 - \eta)\,. \tag{3.1.7}$$

Inserting for the vorticity in (3.1.5), we find that

$$\eta_{tt} - c_0^2(\eta_{xx} + \eta_{yy}) + f^2\eta = f^2\eta_0\,, \tag{3.1.8}$$

where $c_0^2 = gH$, and η_0 is a known function of x and y (the surface elevation at $t = 0$).

The solution to (3.1.8) can be written as a sum of a transient (free) part and a stationary (forced) part

$$\eta = \tilde{\eta}(x, y, t) + \hat{\eta}(x, y)\,, \tag{3.1.9}$$

where $\tilde{\eta}$ and $\hat{\eta}$ fulfils, respectively

$$\tilde{\eta}_{tt} - c_0^2(\tilde{\eta}_{xx} + \tilde{\eta}_{yy}) + f^2\tilde{\eta} = 0\,, \tag{3.1.10}$$

$$-c_0^2(\hat{\eta}_{xx} + \hat{\eta}_{yy}) + f^2\hat{\eta} = f^2\eta_0\,. \tag{3.1.11}$$

Equation (3.1.10) for the transient, free solution is called the *Klein-Gordon* equation and occurs in many branches in physics. Here, it describes long surface waves that are modified by the earth's rotation (Sverdrup or Poincaré waves). These waves will be discussed in the next section. Notice that the initial conditions for the free solution are

$$\tilde{\eta}(x, y, 0) = \eta_0(x, y) - \hat{\eta}(x, y)\,, \tag{3.1.12}$$

and

$$\tilde{\eta}_t = 0\,. \tag{3.1.13}$$

3.2 Geostrophic adjustment

As an example of a stationary solution of (3.1.8), we return to the problem in Section 2.3, where the surface elevation initially was a step function:

$$\eta_0(x) = \begin{cases} h/2, & x > 0, \\ -h/2, & x < 0, \end{cases} \tag{3.2.1}$$

or, for simplicity,

$$\eta_0(x) = \frac{1}{2} h\,\mathrm{sgn}(x), \quad \mathrm{sgn}(x) = \begin{cases} 1, & x > 0, \\ -1, & x < 0. \end{cases} \tag{3.2.2}$$

We assume that the motion is independent of the *y*-coordinate. From (3.1.11) we then obtain

$$\hat{\eta}_{xx} - a^{-2}\hat{\eta} = -\frac{1}{2} a^{-2} h\,\mathrm{sgn}(x)\,. \tag{3.2.3}$$

Here we have defined (for $f > 0$):

$$a = c_0 / f\,, \tag{3.2.4}$$

which is called the barotropic Rossby *radius of deformation*, or simply the barotropic Rossby radius. It sets an important length scale for the influence of rotation in a quasi-homogeneous ocean. The solution of (3.2.3) is easily found to be

$$\hat{\eta} = \frac{1}{2} h\big(1 - \exp(-|x|/a)\big)\mathrm{sgn}(x)\,. \tag{3.2.5}$$

We have sketched this solution in Fig. 3.1

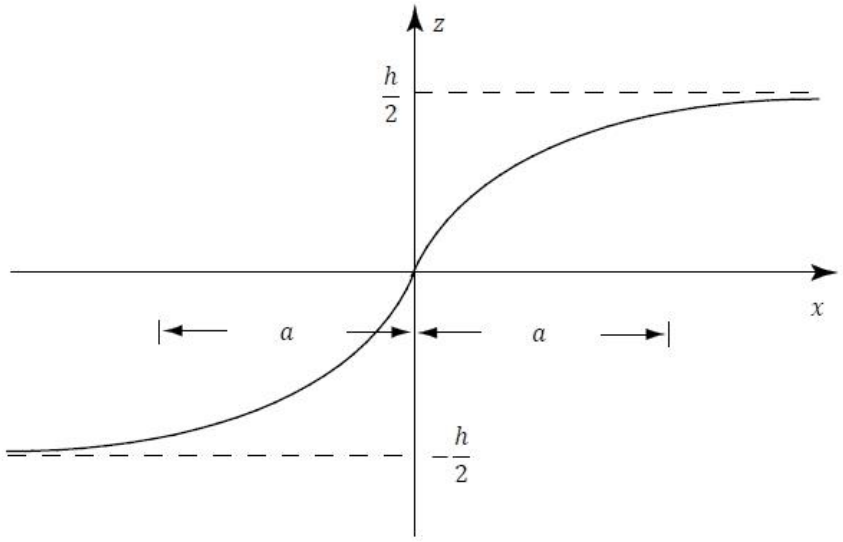

Fig. 3.1 *Geostrophic adjustment of a free surface*.

A typical value for f at mid latitudes is 10^{-4}s^{-1}. For a deep ocean (H = 4000 m), we find from (3.2.4) that $a \approx 2000$ km, while for a shallow ocean (H = 100 m), $a \approx 300$ km.

From (3.1.1) and (3.1.2) we find the velocity distribution for this example, i.e.

$$f\hat{v} = g\hat{\eta}_x\,, \tag{3.2.6}$$

$$\hat{u} = 0\,. \tag{3.2.7}$$

We note from (3.2.6) that we have a balance between the Coriolis force and the pressure-gradient force (geostrophic balance) in the x-direction. Utilizing (3.2.5), the corresponding geostrophic velocity in the y-direction can be written

$$\hat{v} = \frac{gh}{2c_0}\exp(-|x|/a)\,. \tag{3.2.8}$$

This is a "jet"-like stationary flow in the positive y-direction. Although the geostrophic adjustment occurs within the Rossby radius, we notice from (3.2.8) that the maximum velocity in this case is independent of the earth's rotation. By comparison with (2.3.7), we see that our maximum velocity it is the same as the

velocity below a moving pulse with height *h*/2, or as the velocity in the non-rotating step-problem in Section 2.3.

Let us compute the kinetic and the potential energy within a geometrically fixed area $-D \le x \le D$ for the stationary solutions (3.2.5)-(3.2.8), which is valid when $t \to \infty$. The kinetic energy becomes

$$E_k = \frac{1}{2}\rho_0 \int_{-D}^{D} \left(\int_{-H}^{\hat{\eta}} \hat{v}^2 dz \right) dx = \frac{1}{8}\rho_0 g h^2 a(1-e^{-2D/a}), \tag{3.2.9}$$

where we have used the fact that $H >> \overline{\eta}$. For the potential energy we find

$$E_p = \rho_0 g \int_{-D}^{D} \left(\int_{0}^{\hat{\eta}+h/2} z' dz' \right) dx = \frac{1}{2}\rho_0 g h^2 D + \frac{1}{8}\rho_0 g h^2 a(-3+4e^{-D/a} - e^{-2D/a}), \tag{3.2.10}$$

where we have taken $z = -h/2$ as the level of zero potential energy, and introduced $z' = z + h/2$. Initially, the total mechanical energy within the considered area equals the potential energy, or

$$E_0 = E_{p_0} = \frac{1}{2}\rho_0 g h^2 D. \tag{3.2.11}$$

Let us choose *D* >> *a*. We then notice from (3.2.9)-(3.2.11) that

$$E_k + E_p < E_0. \tag{3.2.12}$$

Thus, when $t \to \infty$, the total mechanical energy inside the considered area is *less* than it was at *t* = 0. The reason is that energy in the form of free Sverdrup waves (solutions of the Klein-Gordon equation) has "leaked" out of the area during the adjustment towards a geostrophically balanced steady state. We will consider these waves in more detail in the next section.

Finally we discuss in a quantitative way when it is possible to neglect the effect of earth's rotation on the motion. For this to be possible, we must have that

$$\left|\vec{v}_t\right| >> \left| f\vec{k} \times \vec{v} \right|. \tag{3.2.13}$$

Accordingly, the typical timescale T for the motion must satisfy

$$T << \frac{2\pi}{f}. \tag{3.2.14}$$

At mid latitudes we typically have $2\pi / f \approx 17$ hrs. If the characteristic horizontal scale of the motion is L and the phase speed is $c_0 = (gH)^{1/2}$, we find from (3.2.14) that the effect of earth's rotation can be neglected if

$$L << a. \tag{3.2.15}$$

In the open ocean L will be associated with the wavelength, while in a fjord or canal, L will be the width. Oppositely, when the length scale is larger than the Rossby radius, i.e.,

$$L \geq a, \tag{3.2.16}$$

the effect of the earth's rotation on the fluid motion can *not* be neglected.

3.3 Sverdrup and Poincaré waves

We consider long surface waves in a rotating ocean of unlimited horizontal extent. Such waves are often called Sverdrup waves (Sverdrup, 1927). They are solutions of the Klein-Gordon equation (3.1.10). Actually, Sverdrup's name is usually related to friction-modified, long gravity waves, but here we will use it also for the frictionless case. In literature long waves in an inviscid ocean are often called Poincaré waves. However, this term will be reserved for a particular combination of Sverdrup waves that can occur in canals with parallel walls.

Sverdrup waves

A surface wave component in a horizontally unlimited ocean can be written

$$\eta = A\exp(i(kx + ly - \omega t)). \tag{3.3.1}$$

This wave component is a solution of the Klein-Gordon equation (3.1.10) if

$$\omega^2 = f^2 + c_0^2(k^2 + l^2)\,. \tag{3.3.2}$$

Here *k* and *l* are real wave numbers in the *x*- and *y*-direction, respectively. Equation (3.3.2) is the dispersion relation for inviscid Sverdrup waves. From this relation we note that the Sverdrup wave must always have a frequency that is larger than (or equal to) the inertial frequency *f*.

For simplicity we let the wave propagate along the *x*-axis, i.e. $l = 0$. The phase speed now becomes

$$c = \frac{\omega}{k} = c_0\left(1 + \frac{\lambda^2}{4\pi^2 a^2}\right)^{1/2}, \tag{3.3.3}$$

where λ is the wavelength and *a* is the Rossby radius. We note that the waves become dispersive due to the earth's rotation. The group velocity becomes

$$c_g = \frac{\mathrm{d}\omega}{\mathrm{d}k} = \frac{c_0}{\left(1 + \frac{\lambda^2}{4\pi^2 a^2}\right)^{1/2}}\,. \tag{3.3.4}$$

We notice that the group velocity decreases with increasing wavelength. From (3.3.3) and (3.3.4) we realize that $cc_g = c_0^2$, i.e. the product of the phase and group velocities is constant. From (3.3.2), with $l = 0$, we can sketch the dispersion diagram for positive wave numbers; see Fig. 3.2.

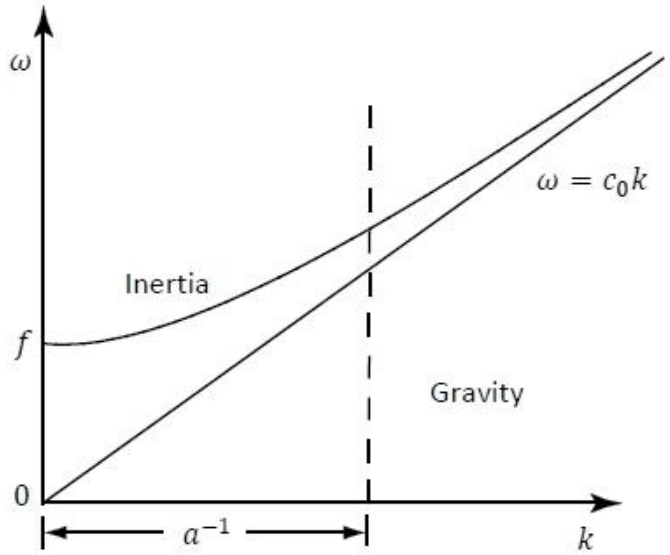

Fig. 3.2 *The dispersion diagram for Sverdrup waves.*

For $k << a^{-1}$ (i.e. $\lambda >> a$) we have that $\omega \approx f$. This means that the motion is reduced to inertial oscillations in the horizontal plane. For $k >> a^{-1}$ gravity dominates, i.e. $\omega \approx c_0 k$, and we have surface gravity waves that are not influenced by the earth's rotation.

Contrary to gravity waves in a non-rotating ocean, the Sverdrup waves discussed here do possess vertical vorticity. For a wave solution ($\propto \exp(i\omega t)$), (3.1.4) yields

$$\zeta = \frac{f}{H}\eta, \tag{3.3.5}$$

where the relative vertical vorticity ζ is defined by (1.4.1). If we still assume that $\partial / \partial y = 0$, we obtain from (3.3.5) and (3.1.2) that

$$\left.\begin{aligned} v_x &= \frac{f}{H}\eta, \\ u &= -\frac{1}{f}v_t. \end{aligned}\right\} \tag{3.3.6}$$

Considering real solutions with

$$\eta = A\cos(kx - \omega t), \tag{3.3.7}$$

we find from (3.3.6):

$$u = \frac{A\omega}{kH}\cos(kx-\omega t),$$
$$v = \frac{Af}{kH}\sin(kx-\omega t), \qquad (3.3.8)$$
$$w = A\omega\left(\frac{z+H}{H}\right)\sin(kx-\omega t).$$

Here the vertical velocity *w* has been obtained from (1.3.8). Since $|\omega| \geq |f|$ for Sverdrup waves, we must have that $|u| \geq |v|$. Furthermore, from (3.3.8) we find that

$$\frac{u^2}{\left(A\omega/(kH)\right)^2} + \frac{v^2}{\left(Af/(kH)\right)^2} = 1. \qquad (3.3.9)$$

This means that the horizontal velocity vector describes an ellipsis where the ratio of the major axis to the minor axis is $|\omega/f|$. From (3.3.8) it is easy to see that the velocity vector turns *clockwise*, and that one cycle is completed in time $2\pi/\omega$.

Sverdrup (1927) demonstrated that the tidal waves on the Siberian continental shelf were of the same type as the waves discussed here. In addition, they were modified by the effect of bottom friction, which leads to a damping of the wave amplitude as the wave progresses. Furthermore, friction acts to reduce of the phase speed, and it causes a phase displacement between maximum current and maximum surface elevation.

In this connection it is interesting to consider the most energetic tidal constituent in the Barents Sea region, which is M_2. This tidal component has a period $T = 12.42$ hrs, and the corresponding frequency becomes $\omega = 1.41\times10^{-4}\,\mathrm{s}^{-1}$. According to the results above, it can only exist as a free Sverdrup wave if $\omega \geq f = 2\Omega\sin\varphi$. This means that we have a critical latitude $\varphi_c = \sin^{-1}(\omega/2\Omega)$, or $\varphi_c = 75^{\circ}2.8'$ N, for this component. At higher latitudes than φ_c, the M_2 component cannot exist as a Sverdrup wave. However, we shall discover later on that this

component indeed can exist at higher latitudes, but then in the form of a *coastal Kelvin* wave, to be discussed in Section 3.5.

Poincaré waves

We consider waves in a uniform canal along the *x*-axis with depth *H* and width *B*. Such waves must satisfy the Klein-Gordon equation (3.1.10). But now the ocean is laterally limited. At the canal walls, the normal velocity must vanish, i.e. $v = 0$ for $y = 0, B$. By inspecting (3.3.8), we realize that no single Sverdrup wave can satisfy these conditions. However, if we superimpose *two* Sverdrup waves, both propagating at oblique angles (α and $-\alpha$, say) with respect to the *x*-axis, we can construct a wave which satisfies the required boundary conditions. The velocity component in the *y*-direction must then be of the form

$$v = v_0 \sin(\frac{n\pi y}{B}) \exp(i(kx - \omega t)), \quad n = 1,2,3,.. \tag{3.3.10}$$

Since the wave number $l = n\pi / B$ in the *y*-direction now is discrete due to the boundary conditions, the dispersion relation (3.3.2) becomes

$$\omega = \pm \left[f^2 + c_0^2 \left(k^2 + \frac{n^2 \pi^2}{B^2} \right) \right]^{1/2}, \quad n = 1,2,3,... \tag{3.3.11}$$

We notice from (3.3.10) that the spatial variation in the cross-channel direction is trigonometric. Such trigonometric waves in a rotating channel are called *Poincaré waves*. They can propagate in the positive as well as the negative *x*-direction. We shall see that this is in contrast to coastal Kelvin waves, which we discuss later in this section. In general, the derivation of the complete solution for Poincaré waves is too lengthy to be discussed in this text. For a detailed derivation; see for example LeBlond and Mysak (1978), p. 270.

3.4 Energy flux in Sverdrup waves

We have previously, in Section 2.5, calculated the mean energy flux in surface waves without rotation. It is interesting to do a similar calculation for shallow-water waves in a rotating ocean. By utilizing the solutions (3.3.7)-(3.3.8), we can compute the mechanical energy associated with Sverdrup waves. The mean potential energy per unit area of a fluid column can be written

$$E_p = \frac{1}{T}\int_0^T (\rho_0 g \int_0^\eta z dz) dt = \frac{1}{4} g \rho_0 A^2, \tag{3.4.1}$$

where $T = 2\pi/\omega$. The mean kinetic energy per unit area becomes

$$E_k = \frac{1}{T}\int_0^T \frac{1}{2}\rho_0 \left(\int_{-H}^0 (u^2 + v^2 + w^2) dz \right) dt = \frac{1}{4} g \rho_0 \left[\frac{1 + f^2/\omega^2}{1 - f^2/\omega^2} \right] A^2, \tag{3.4.2}$$

where we have utilized that $kH << 1$. We see that in a rotating ocean ($f \neq 0$), the mean potential and the mean kinetic energy in the wave motion are no longer equal. This is in contrast to the non-rotating case, e.g. (3.6.3), where we have an equal partition between the two. The dominating part of the mean energy is now kinetic. The energy density becomes

$$E = E_k + E_p = \frac{1}{2}\rho_0 g A^2 c^2 / c_0^2. \tag{3.4.3}$$

Consider a Sverdrup wave that propagates along *x*-axis. This wave induces a net transport of energy in the *x*-direction. The mean horizontal energy flux is the work per unit time by the dynamic (fluctuating) pressure in displacing particles horizontally. In shallow water the dynamic pressure is $p = \rho_0 g \eta$. The mean energy flux to second order in wave amplitude can then be written

$$F_e = \frac{1}{T}\int_0^T \rho_0 g \left(\int_{-H}^0 \eta u dz \right) dt. \tag{3.4.4}$$

Inserting from (3.3.7) and (3.3.8), it follows that

$$F_e = \frac{1}{2}\rho_0 gcA^2 = \frac{c_0^2}{c}E = c_g E\,. \tag{3.4.5}$$

As could be expected, also in Sverdrup waves the mean energy propagates with the group velocity. This is in fact a quite general result for wave motion.

In this case it is very simple to derive the concepts of energy density and energy flux directly from the energy equation for the fluid. With no variation in the *y*-direction, the linearized equations (3.1.1)-(3.1.3) reduce to

$$\left.\begin{aligned} u_t - fv &= -g\eta_x, \\ v_t + fu &= 0, \\ \eta_t &= -Hu_x. \end{aligned}\right\} \tag{3.4.6}$$

By multiplying the two first equations by *u* and *v*, respectively, and then adding, we obtain

$$\frac{\partial}{\partial t}\left[\frac{1}{2}(u^2+v^2)\right] = -\frac{\partial}{\partial x}(gu\eta) + gu_x\eta\,. \tag{3.4.7}$$

Obviously, the Coriolis force does not perform any work since it acts perpendicular to the displacement (or the velocity). By inserting that $u_x = -\eta_t / H$ into the last term, (3.4.7) becomes

$$\frac{\partial}{\partial t}\left[\frac{1}{2}\rho_0\left(u^2+v^2+\frac{g}{H}\eta^2\right)\right] + \frac{\partial}{\partial x}(\rho_0 g\eta u) = 0\,. \tag{3.4.8}$$

We write this equation

$$\frac{\partial}{\partial t}e_d + \frac{\partial}{\partial x}e_f = 0\,, \tag{3.4.9}$$

where the energy density e_d and the energy flux e_f per unit volume are defined, respectively, as

$$e_d = \frac{1}{2}\rho_0\left(u^2+v^2+\frac{g}{H}\eta^2\right), \tag{3.4.10}$$

$$e_f = \rho_0 g\eta u\,. \tag{3.4.11}$$

The mean values for a vertical fluid column become, not unexpectedly:

$$\left.\begin{aligned} \frac{1}{T}\int_0^T\Big(\int_{-H}^0 e_d\,dz\Big)dt &= \frac{1}{2}\frac{\rho_0 g c^2 A^2}{c_0^2} = E, \\ \frac{1}{T}\int_0^T\Big(\int_{-H}^0 e_f\,dz\Big)dt &= \frac{1}{2}\rho_0 g c A^2 = F_e, \end{aligned}\right\} \tag{3.4.12}$$

where $F_e = c_g E$.

3.5 Coastal Kelvin waves

We consider an ocean that is limited by a straight coast. The coast is situated at $y = 0$; see Fig. 3.3.

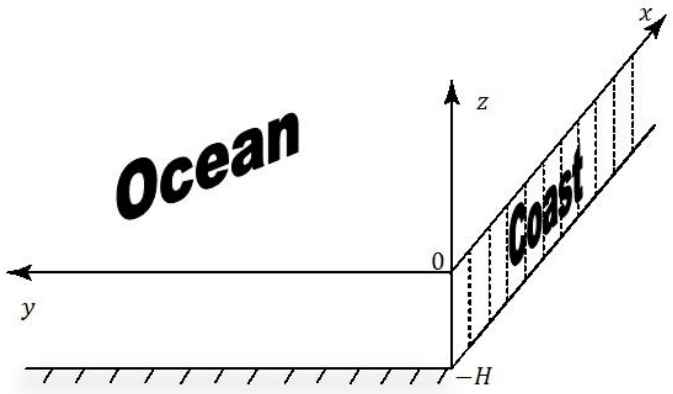

Fig. 3.3 *Definition sketch.*

Furthermore, we assume that the velocity component in the *y*-direction is zero everywhere, i.e. $v \equiv 0$. With constant depth and constant surface pressure (3.1.1)-(3.1.3) become

$$u_t = -g\eta_x\,, \tag{3.5.1}$$

$$fu = -g\eta_y\,, \tag{3.5.2}$$

$$\eta_t = -Hu_x\,. \tag{3.5.3}$$

We take that the Coriolis parameter is constant, and eliminate *u* from the problem. Equations (3.5.1) and (3.5.2) yield

$$\eta_{yt} - f\eta_x = 0\,, \tag{3.5.4}$$

while (3.5.2) and (3.5.3) yield

$$\eta_t - ac_0\eta_{xy} = 0\,, \tag{3.5.5}$$

where c_0 is the shallow water speed and a is the Rossby radius. We assume a solution of the form

$$\eta = G(y)F(x,t)\,. \tag{3.5.6}$$

By inserting into (3.5.5), we find

$$\frac{F_t}{c_0 F_x} = \frac{aG'}{G}\,, \tag{3.5.7}$$

where $G' = dG/dy$. The left-hand side of (3.5.7) is only a function of x and t, and the right-hand side is only a function of y. Thus, for (3.5.7) to be valid for arbitrary values of x, y, and t, both sides must equal to the same constant, which we denote by γ ($\gamma \neq 0$ for a non-trivial solution). Hence

$$\begin{aligned} \frac{aG'}{G} = \gamma \quad &\Rightarrow \quad G = \exp(\gamma y/a), \\ \frac{F_t}{c_0 F_x} = \gamma \quad &\Rightarrow \quad F = F(x + \gamma c_0 t). \end{aligned} \tag{3.5.8}$$

By inserting from (3.5.8) into (3.5.4), we find that

$$\gamma = \pm 1\,. \tag{3.5.9}$$

Accordingly, from (3.5.8), we have solutions of the form

$$\eta = \exp(y/a)F(x + c_0 t)\,, \tag{3.5.10}$$

and

$$\eta = \exp(-y/a)F(x - c_0 t)\,. \tag{3.5.11}$$

If we have a straight coast at $y = 0$ and an unlimited ocean for $y > 0$, as depicted in Fig. 3.3, the solution (3.5.10) must be discarded. This is because η must be *finite*

everywhere in the ocean, even when $y \to \infty$. The solution for the surface elevation and the velocity distribution in this case then become

$$\eta = \exp(-y/a)F(x - c_0 t),$$
$$u = \frac{g}{fa}\exp(-y/a)F(x - c_0 t). \tag{3.5.12}$$

This type of wave is called a single *Kelvin* wave (double Kelvin waves will be treated in section 3.8). It is *trapped* at the coast within a region determined by the Rossby radius. It is therefore also referred to as a *coastal* Kelvin wave. The Kelvin wave propagates in the positive x-direction with velocity c_0, like a gravity wave without rotation. The difference from the non-rotating case, however, is that now we do not have the possibility of a wave in the negative x-direction. This is because the Kelvin wave solution requires geostrophic balance in the direction *normal* to the coast; see (3.5.2). This is impossible for a wave in the negative x-direction in the northern hemisphere. In general, if we look in the direction of wave propagation (along the wave number vector), a Kelvin wave in the northern hemisphere always moves with the coast to the right, while in the southern hemisphere ($f < 0$), it moves with the coast to the left; see the sketch in Fig. 3.4 for a single Fourier component in the northern hemisphere.

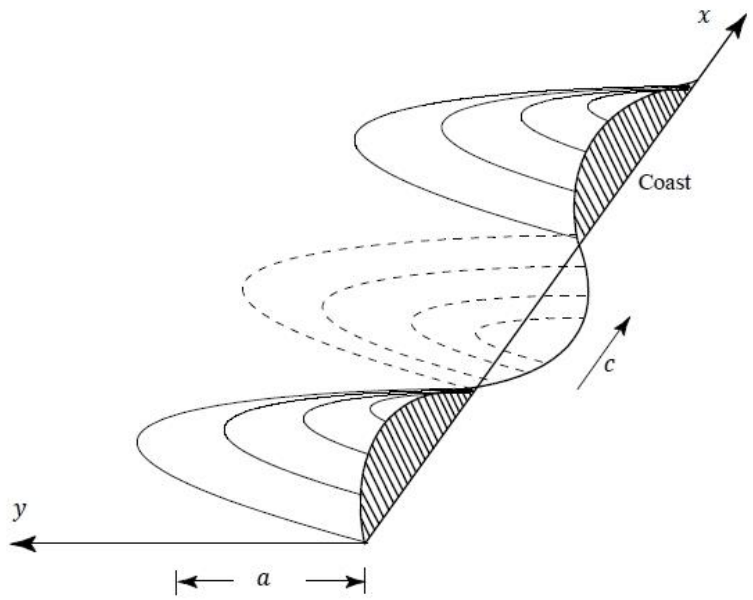

Fig. 3.4 *Propagation of Kelvin waves along a straight coast when f > 0.*

Since the wave amplitude is trapped within a region limited by the Rossby radius, the wave energy is also trapped in this region. The energy propagation velocity (the group velocity) is here $c_g = d\omega/dk = d(c_0 k)/dk = c_0$, and the energy is propagating with the coast to the right in the northern hemisphere. We note that for Kelvin waves the frequency has not a lower limit (for Sverdrup waves $\omega \geq f$).

The oceanic tide may in certain places manifest itself as coastal Kelvin waves of the type studied here. We will discuss this further in connection with amphidromic points (points where the tidal height is always zero).

From (3.5.12) we notice that the surface elevation and velocity are in phase, i.e. maximum high tide coincides with maximum current. It turns out from measurements that the maximum tidal current at a given location occurs *before* maximum tidal height. This is due to the effect of friction at the ocean bottom, which we have

neglected so far. In order to include the effect of friction in the simplest possible way, we model the friction force as in (1.1.7). The linearized *x*-component now becomes

$$u_t = -g\eta_x - ru\,. \tag{3.5.13}$$

Since $v = 0$, (3.5.2) and (3.5.3) remain as before. By eliminating *u* between (3.5.13) and (3.5.3), we obtain

$$\eta_{tt} - gH\eta_{xx} + r\eta_t = 0\,. \tag{3.5.14}$$

We now assume a solution in terms of the complex Fourier component

$$\eta = G(y)\exp(i(\kappa x - \omega t))\,. \tag{3.5.15}$$

Here ω is real, while the wave number κ in the *x*-direction is complex:

$$\kappa = k + i\alpha\,. \tag{3.5.16}$$

We take that $k > 0$ is the real wave number, while α is the spatial damping coefficient in the *x*-direction. We shall assume throughout this analysis that $|\alpha| << k$, i.e. the wave damping is small over a distance comparable to the wavelength. Inserting (3.5.15) into (3.5.14), we obtain the complex dispersion relation

$$\omega^2 + ir\omega - gH\kappa^2 = 0\,. \tag{3.5.17}$$

Utilizing that $|\alpha|/k << 1$, the real part of (3.5.17) yields to lowest order that $\omega = \pm(gH)^{1/2}k$, as before. We consider waves that propagate in the positive *x*-direction, i.e. $\omega = (gH)^{1/2}k = c_0 k$. From the imaginary part of (3.5.17) we then obtain

$$\alpha = \frac{r}{2c_0}\,. \tag{3.5.18}$$

The value of *r* depends, among other things, on the bottom roughness. A typical value derived from the tidal literature could be $r \sim 2.5\times10^{-5}\,\mathrm{s}^{-1}$.

The geostrophic balance condition in (3.5.2) now yields

$$\frac{dG}{dy}+\left(\frac{1}{a}-il\right)G=0, \tag{3.5.19}$$

where $l=\alpha/(ka)$ is a small wave number in the *y*-direction induced by the combined action of friction and rotation. This yields a coastally trapped solution:

$$G=A\exp(-y/a)\exp(ily). \tag{3.5.20}$$

If we let the real part represent the physical solution, we then obtain for this case

$$\begin{aligned}\eta &= A\exp(-\alpha x-y/a)\cos(kx+ly-\omega t),\\ u &= \frac{c_0 A}{H}\exp(-\alpha x-y/a)\left(\cos(kx+ly-\omega t)+\frac{\alpha}{k}\sin(kx+ly-\omega t)\right).\end{aligned} \tag{3.5.21}$$

We note from this solution that at a given location, ($x=0, y=0$) say, the current maximum is ahead in time of the surface elevation maximum, as known from observations. We also note that the lines describing a constant phase (the co-tidal lines) are no longer directed perpendicular to the coast, but are slanting backwards relative to the direction of wave propagation (Martinsen and Weber, 1981). This situation is sketched in Fig. 3.5:

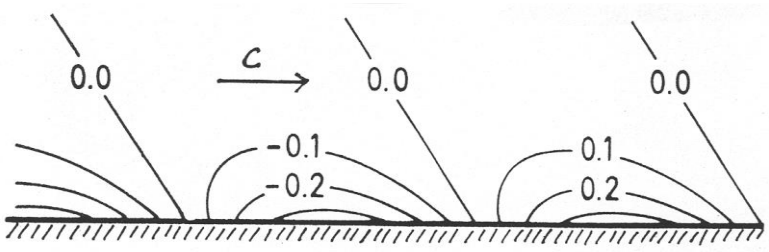

Fig. 3.5 *Coastal Kelvin waves influenced by friction. Here* $c=c_0$ *is the phase speed in the x-direction.*

3.6 Amphidromic systems

Wave systems, where the lines of constant phase, or the *co-tidal* lines, form a star-shaped pattern, are called *amphidromies*. They are wave interference phenomena, and

in the ocean they usually originate due to interference between Kelvin waves. Let us study wave motion in an ocean with width *B*; see the sketch in Fig. 3.6.

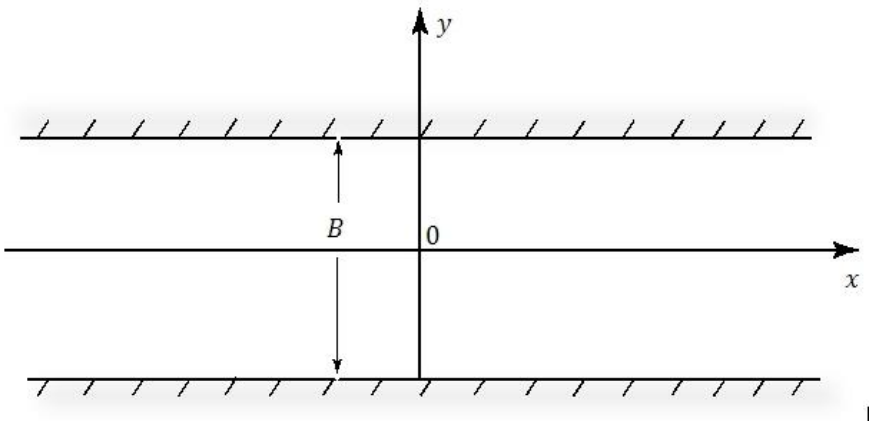

Fig. 3.6 *Ocean with parallel boundaries (infinitely long channel).*

Since the ocean now is limited in the *y*-direction, *both* Kelvin wave solutions (3.5.10) and (3.5.11) can be realized. Because we are working with linear theory, the sum of two solutions is also a solution, i.e.

$$\eta = \exp(y/a)F(x+c_0t) + \exp(-y/a)F(x-c_0t)\,. \tag{3.6.1}$$

In general the *F*-functions in (3.6.1) can be written as sums of Fourier components. It suffices here to consider two Fourier components with equal amplitudes:

$$\eta = A\big(\exp(y/a)\sin(kx+\omega t) + \exp(-y/a)\sin(kx-\omega t)\big), \tag{3.6.2}$$

where $\omega = c_0k$. Along the *x*-axis, i.e. for $y = 0$, (3.6.2) reduces to

$$\eta = 2A\sin kx\cos\omega t\,. \tag{3.6.3}$$

This constitutes a standing oscillation with period $T = 2\pi/\omega$. Zero elevation ($\eta = 0$) occurs when

$$x = \frac{n\pi}{k}, \quad n = 0,1,2,... \tag{3.6.4}$$

At the locations given by $(n\pi/k, 0)$, the surface elevation is zero at all times. These nodal points are referred to as *amphidromic* points.

We consider the shape of the co-phase lines, and choose a particular phase, e.g. a wave crest (or trough). At a given time the spatial distribution of this phase is given by $\eta_t = 0$; i.e. a local extreme for the surface elevation. Partial differentiation (3.6.2) with respect to time yields that the co-phase lines are given by the equation

$$\exp(y/a)\cos(kx+\omega t) - \exp(-y/a)\cos(kx-\omega t) = 0\,. \qquad (3.6.5)$$

We notice right away that the co-phase lines must intersect at the amphidromic points $x = n\pi/k,\ y = 0$ for all times. As an example, we consider the amphidromic point at the origin. In a sufficiently small distance from origin, *x* and *y* are so small that we can make the approximations $\exp(\pm y/a) \approx 1 \pm y/a, \cos kx \approx 1, \sin kx \approx kx$. Equation (3.6.5) then yields

$$y = (ka\tan\omega t)x\,. \qquad (3.6.6)$$

This means that the co-phase lines are straight lines in a region sufficiently close to the amphidromic points. Since $\tan\omega t$ is a monotonically increasing function of time in the interval $t = 0$ to $t = \pi/(2\omega)$, we see that a co-phase line revolves around the amphidromic point in a *counter-clockwise* direction in this example $(f > 0)$. It turns out that, as a main rule, the co-phase lines of the amphidromic systems in the world oceans rotate counter-clockwise in the northern hemisphere and clockwise in the southern hemisphere. We notice from (3.6.6) that if we have high tide along a line in the region $x > 0$, $y > 0$ at some time *t*, we will have high tide along the same line in the region $x < 0$, $y < 0$ at time $t + \pi/\omega$, or half a period later.

We now consider the numerical value of η along a co-phase line. Close to an amphidromic point, (here the origin), we can use (3.6.2) to express the elevation as

$$\eta = 2A(kx\cos\omega t + \frac{y}{a}\sin\omega t)\,. \tag{3.6.7}$$

From (3.6.6) we find that $\tan\omega t = y/(kax)$ along a co-phase line. By eliminating the time dependence between this expression and (3.6.7), we find for the magnitude of the surface elevation along a co-tidal line:

$$|\eta| = 2A\left(k^2x^2 + y^2/a^2\right)^{1/2}. \tag{3.6.8}$$

The lines for a given difference between high and low tide are called *co-range* lines. These curves are given by (3.6.8), when $|\eta|$ is put equal to a constant, i.e.

$$k^2x^2 + y^2/a^2 = \text{const.} \tag{3.6.9}$$

We thus see that the co-range lines close to the amphidromic points are ellipses.

In Fig. 3.7 we have depicted co-phase lines (solid curves) and co-range lines (broken curves) resulting from the superposition of two oppositely travelling Kelvin waves, both with periods of 12 hours and amplitudes of 0.5 m. The wavelength is 800 km, the width of the channel is 400 km, the depth is 40 m, and the Coriolis parameter is 10^{-4}s^{-1}. The Rossby radius becomes 198 km in this example. Hence the right-hand side of the channel is dominated by the upward-propagating Kelvin wave (the one with minus sign in the phase), and the left-hand side is dominated by the downward propagating Kelvin wave.

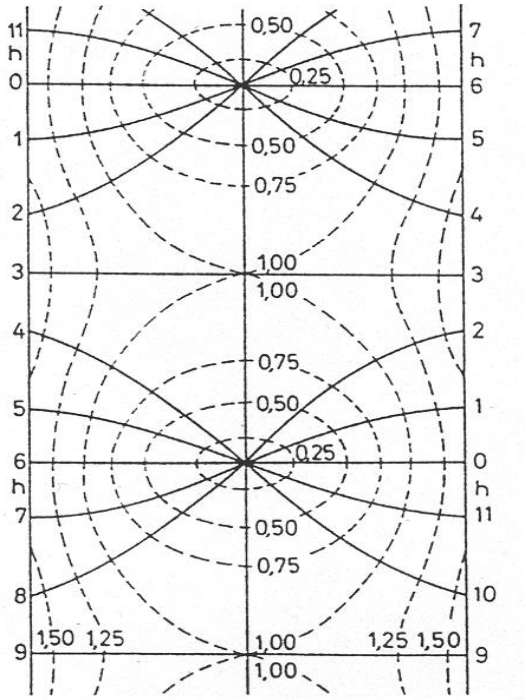

Fig. 3.7 *Amphidromic system in an infinitely long channel.*

3.7 Equatorial Kelvin waves

Close to equator we have that $f_0 \approx 0$. From (1.1.2) the Coriolis parameter in this region can then be approximated by

$$f = \beta y . \tag{3.7.1}$$

where the *y*-axis is directed northwards; see Fig. 3.8.

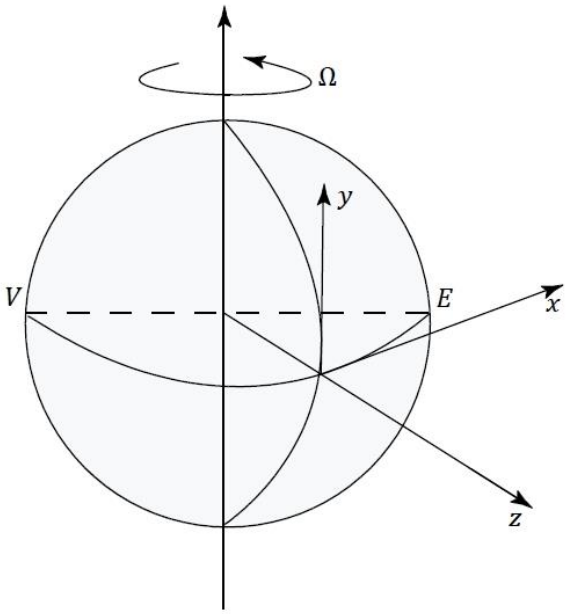

Fig. 3.8 *Sketch of the co-ordinate axes near the equator*.

We shall find that it is possible to have equatorially trapped gravity waves, analogous to the trapping at a straight coastline. Assume that the velocity component in the *y*-direction is zero everywhere, i.e. we assume geostrophic balance in the direction perpendicular to equator. With constant depth, the equations (3.5.1)-(3.5.3) are unchanged, but now $f = \beta y$ in (3.5.2). By assuming a solution of the form $\eta = G(y)F(x,t)$ as before, (3.5.7) becomes

$$\frac{F_t}{c_0 F_x} = \frac{c_0 G'}{\beta y G} = \gamma \,. \tag{3.7.2}$$

Accordingly:

$$\left.\begin{aligned} F &= F(x + \gamma c_0 t), \\ G &= \exp\left(\frac{\gamma\beta}{2c_0} y^2\right). \end{aligned}\right\} \tag{3.7.3}$$

By inserting into (3.5.4), we find

$$\gamma = \pm 1 \,. \tag{3.7.4}$$

From (3.7.3) we realize that to have finite solution when $y \to \pm\infty$, we must choose $\gamma = -1$ in (3.7.4). The solution thus becomes

$$\left.\begin{aligned} \eta &= \exp(-y^2/a_e^2)F(x-c_0t), \\ u &= \frac{g}{c_0}\exp(-y^2/a_e^2)F(x-c_0t), \end{aligned}\right\} \tag{3.7.5}$$

where the *equatorial* Rossby radius a_e is defined by

$$a_e = (2c_0/\beta)^{1/2}. \tag{3.7.6}$$

We note that the solution (3.7.5), referred to as an *equatorial* Kelvin wave, is valid at both sides of equator and that it propagates in the positive *x*-direction, i.e. *eastwards* with phase speed $c_0 = (gH)^{1/2}$. The energy also propagates eastwards with the same velocity, since we have no dispersion. At the equator β is approximately $2\times10^{-11}\mathrm{m}^{-1}\mathrm{s}^{-1}$. For a deep ocean with $H = 4000\ \mathrm{m}$, we find from (3.7.6) that the equatorial Rossby radius becomes about 4500 km.

Equatorial Kelvin waves are generated by tidal forces, and by wind stress and pressure distributions associated with storm events with horizontal scales of thousands of kilometres. When such waves meet the eastern boundaries in the ocean (the west coast of the continents), part of the energy in the wave motion will split into a northward propagating coastal Kelvin waves in the northern hemisphere, and a southward propagating coastal Kelvin wave in the southern hemisphere. Some of the energy may also be reflected in the form of long planetary Rossby waves (in such waves the energy propagates westward if the wavelength is much larger than the Rossby radius).

3.8 Topographically trapped waves

We have seen that gravity waves can be trapped at the coast or at the equator due to the effect of the earth's rotation. Trapping of wave energy in a rotating ocean can also occur in places where we have changes in the bottom topography. In this case, however, the wave motion is fundamentally different from that associated with Kelvin waves. While the velocity field induced by Kelvin waves is always zero in a direction perpendicular to the coast, or equator, it is in fact the displacement of particles perpendicular to the bottom contours that generates waves in a region with sloping bottom. We call these waves *escarpment* waves, and they arise as a consequence of the conservation of potential vorticity.

Rigid lid

The escarpment waves are essentially vorticity waves. The motion in these waves is a result of the conservation of potential vorticity. More precisely, the relative vorticity for a vertical fluid column changes periodically in time when the column is stretched or squeezed in a motion back and forth across the bottom contours. To study such waves in their purest form, we will assume that the surface elevation is zero at all times, i.e. we apply the rigid lid approximation. In this way the effect of gravity is eliminated from the problem. Let us assume that the bottom topography is as sketched in Fig. 3.9.

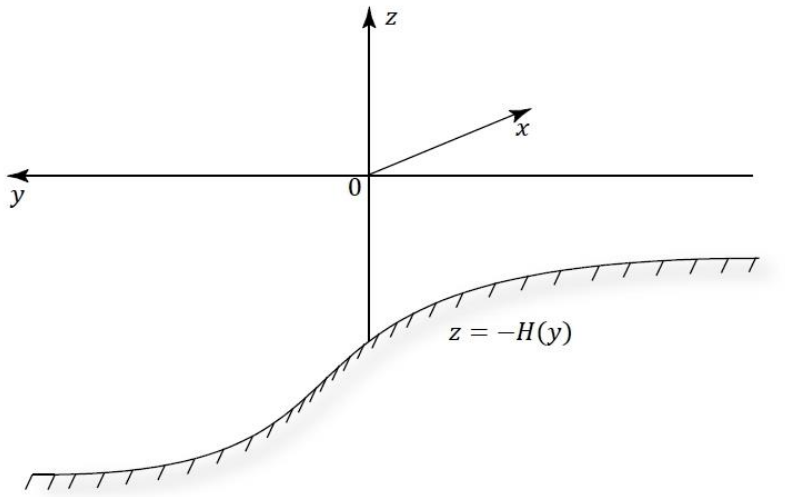

Fig. 3.9 *Bottom topography for escarpment waves*.

The linearized continuity equation (1.3.12) can now be written as

$$(Hu)_x + (Hv)_y = 0\,. \tag{3.8.1}$$

Accordingly, we can define a stream function ψ satisfying

$$\left.\begin{aligned} Hu &= -\psi_y, \\ Hv &= \psi_x. \end{aligned}\right\} \tag{3.8.2}$$

When linearizing, we obtain from the theorem of conservation of potential vorticity (1.4.5) that

$$\frac{\zeta_t}{H} + u\left(\frac{f}{H}\right)_x + v\left(\frac{f}{H}\right)_y = 0\,. \tag{3.8.3}$$

We here assume that *f* is constant. Furthermore, we take that $H = H(y)$. By inserting ψ from (3.8.2), we can write (3.8.3) as

$$\nabla^2\psi_t - \frac{H'}{H}(\psi_{yt} + f\psi_x) = 0\,, \tag{3.8.4}$$

where $H' = dH/dy$. We assume a wave solution of the form

$$\psi = F(y)\exp(i(kx - \omega t))\,. \tag{3.8.5}$$

By inserting into (3.8.4), this yields

$$\left(\frac{F'}{H}\right)' - \left(\frac{k^2}{H} - \frac{kf}{\omega}\frac{H'}{H^2}\right)F = 0\,. \tag{3.8.6}$$

This equation has non-constant coefficients and is therefore problematic to solve for a general form of $H(y)$. We shall not make any attempts to do so here. Instead, we derive solutions for two extreme types of bottom topography. One of these cases, where the bottom exhibits a weak exponential change in the y-direction, will be dealt with in sec 3.9 in connection with topographic Rossby waves. The other extreme case, where the slope tends towards a step function, will be analysed here; see the sketch in Fig. 3.10. The escarpment waves relevant for this topography are often called *double* Kelvin waves.

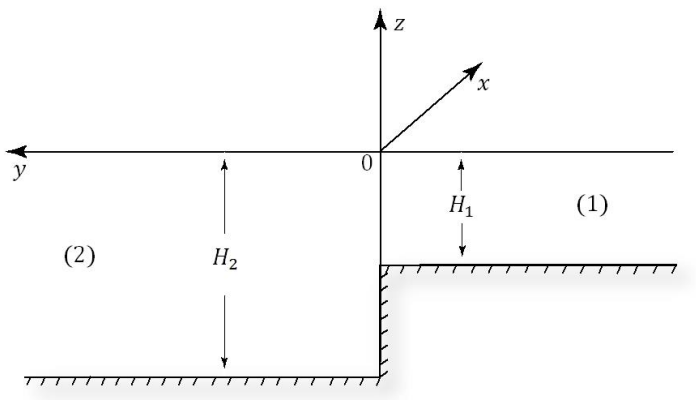

Fig. 3.10 *The bottom configuration for double Kelvin waves*.

For *trapped* waves, the solutions of (3.8.6) in areas (1) and (2) are, respectively

$$\left.\begin{aligned} F_1 &= A_1 \exp(ky), \\ F_2 &= A_2 \exp(-ky). \end{aligned}\right\} \tag{3.8.7}$$

We note that these waves are trapped within a distance of one wavelength on each side of the step. At the step itself ($y = 0$), the volume flux in the y-direction must be continuous, i.e.

$$v_1 H_1 = v_2 H_2, \quad y = 0. \tag{3.8.8}$$

This means that ψ_x (and thereby also ψ) must be continuous for $y = 0$, i.e. $A_1 = A_2 = A$ in (3.8.7). Furthermore, the pressure in the fluid must be continuous for $y = 0$. The pressure is obtained from the linearized x-component of (1.1.1) in the absence of friction, i.e.

$$p_x = -\rho(u_t - fv) = -\frac{\rho}{H}\left((Hu)_t - fHv\right). \tag{3.8.9}$$

Writing $p = P(y)\exp(i(kx - \omega t))$, and applying (3.8.2) and (3.8.5), we find that

$$P = \rho\left(-\frac{\omega F'}{kH} + \frac{fF}{H}\right). \tag{3.8.10}$$

By inserting from (3.8.7), with $A_1 = A_2$, into (3.8.10), continuity of the pressure at $y = 0$ yields the dispersion relation

$$\omega = f\left[\frac{H_2 - H_1}{H_2 + H_1}\right]. \tag{3.8.11}$$

We note that we always have that $|\omega| < |f|$, and that the wave propagates with shallow water to the right in the northern hemisphere, i.e. $\omega > 0$ when $f > 0$. These two properties are generally valid for escarpment waves, even though we have only shown it for double Kelvin waves with a rigid lid on top.

In the case where the escarpment represents the transition between a continental shelf of finite width and the deep ocean, this type of waves are often called *continental shelf* waves. This kind of bottom topography is found outside the coast of Western Norway. Here, numerical results show the existence of continental shelf waves in the area close to the shelf-break, e.g. Martinsen, Gjevik and Røed (1979). The topographic trapping of long waves near the shelf-break and the currents associated with these waves, interact with the wind-generated surface waves, which

tend to make the sea state here particularly rough. This is a well-known fact among fishermen and other sea travellers that frequent this region.

The effect of gravity

In general, we must allow the sea surface to move vertically. Let us consider a wave solution of the form

$$(u,v,\eta) \propto \exp(i(kx-\omega t)). \tag{3.8.12}$$

For such waves, the linear versions of (1.3.10) and (1.3.11), with constant surface pressure, yield

$$\left.\begin{aligned} u &= -\frac{g}{f^2-\omega^2}\left(k\omega\eta + f\eta_y\right), \\ v &= \frac{ig}{f^2-\omega^2}\left(kf\eta + \omega\eta_y\right). \end{aligned}\right\} \tag{3.8.13}$$

We write the surface elevation as

$$\eta = G(y)\exp(i(kx-\omega t)). \tag{3.8.14}$$

Inserting into the linear version of (1.3.12), we find

$$(HG')' + \left[\frac{\omega^2-f^2}{g} - k^2H + \frac{fk}{\omega}H'\right]G = 0. \tag{3.8.15}$$

For $\omega^2 << f^2$, i.e. quasi-geostrophic motion, we revert to the gravity-modified escarpment wave. For $f = 0$ and $H = (\tan\alpha)y$, this equation yields edge waves, as treated in Section 2.6.

3.9 Topographic Rossby waves

Let us assume that somewhere the relative vorticity is zero. From the theorem of conservation of potential vorticity (1.4.10) with $\eta \equiv 0$, we find that a displacement northwards, where f is increasing, generates negative (anti-cyclonic) relative vorticity.

However, we realize that the same effect can be achieved by a northward displacement if *f* is constant and the depth *H decreases* northward. This gives rise to the so-called *topographic* Rossby waves. Of course, the existence of such waves does not require that the bottom does slope in one particular direction.

Topographic Rossby waves are only a special case of escarpment waves when the bottom has a very weak exponential slope. For comparison with the planetary case, we let the depth decrease northwards, i.e. $H = H_0 \exp(-\alpha y)$, where $\alpha > 0$. Equation (3.8.6) then reduces to

$$F'' + \alpha F' - \left(k^2 + \frac{\alpha f k}{\omega} \right) F = 0 . \qquad (3.9.1)$$

By assuming

$$F = A \exp(i \kappa y) , \qquad (3.9.2)$$

insertion into (3.9.1) yields the complex dispersion relation

$$-i\alpha\kappa + k^2 + \kappa^2 + \frac{\alpha f k}{\omega} = 0 . \qquad (3.9.3)$$

In general we may allow for a very weak change of wave amplitude in the direction normal to the coast, i.e. we take κ in (3.9.2) to be complex:

$$\kappa = l + i\gamma . \qquad (3.9.4)$$

By insertion into (3.9.3), the imaginary part leads to $\gamma = \alpha / 2$ (when $l \neq 0$). From the real part of (3.9.3) we then obtain

$$\omega = -\frac{\alpha f k}{k^2 + l^2 + \alpha^2 / 4} . \qquad (3.9.5)$$

We note that the phase speed component $c^{(x)} = \omega / k$ along the bottom contours is negative. This means that the wave propagation in this direction is such that we have shallow water to the right (in the northern hemisphere).

For a bottom that slopes gently compared to the wavelength $(k >> \alpha)$, we see from the (3.9.5) that these waves are similar to short planetary waves propagating in a fluid of constant depth. On a β-plane we have the familiar dispersion relation

$$\omega = -\frac{\beta k}{k^2 + l^2}\,. \tag{3.9.6}$$

We note that the expressions for the frequency ω are identical in (3.9.5) and (3.9.6), if

$$\beta = \alpha f\,. \tag{3.9.7}$$

This similarity is often used in laboratory experiments in order to simulate planetary effects. When $l = 0$, the equations are satisfied for $\gamma = 0$, i.e. constant amplitude waves. Such waves propagate along the bottom contours with shallow water to the right, and mimic short planetary Rossby waves along latitudinal circles in an ocean of constant depth. We should remember, however, that the energy in such waves $(k >> \alpha, l = 0)$ propagates in the opposite direction, i.e. $c_g = d\omega/dk = \alpha f / k^2 > 0$.

IV. SHALLOW-WATER WAVES IN A STRATIFIED ROTATING OCEAN

4.1 Two-layer model

We now proceed to study the effect of vertical density stratification in the ocean. In many situations the density is approximately constant in a layer close to the surface, while the density in the deeper water is also are constant (and larger). The transition zone between the two layers is called the *pycnocline*. Thin pycoclines are typically found in many Norwegian fjords. In extreme cases we can imagine that the pycnocline thickness approaches zero, resulting in a two-layer model with a jump in the density across the interface between the layers.

We start out by studying such a model. For simplicity we describe the motion in reference system as shown in Fig. 4.1, where the *x*-axis is situated at the undisturbed

interface between the layers. The constant density in each layer is ρ_1 and ρ_2, respectively, where $\rho_2 > \rho_1$.

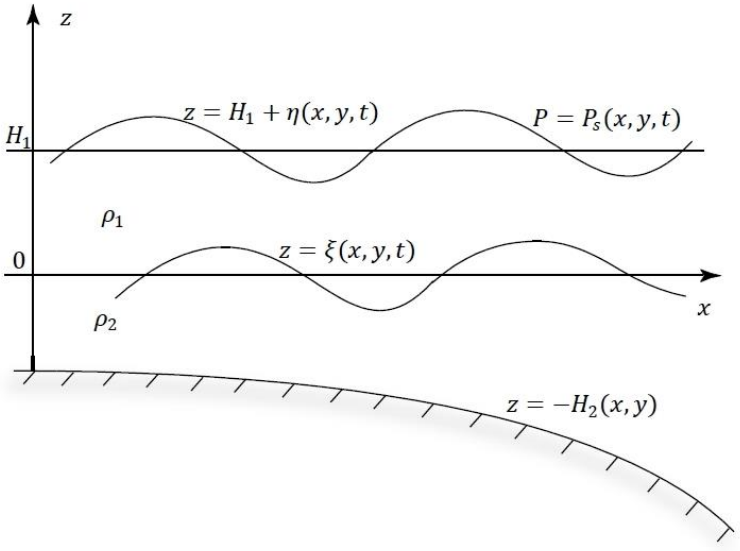

Fig. 4.1 *Model sketch of the two-layer system.*

We assume hydrostatic pressure distribution in each layer. By applying that the pressure is P_S along the surface, and continuous at the interface, i.e. $p_1(z = \xi) = p_2(z = \xi)$, we find that

$$\left.\begin{aligned} p_1 &= -\rho_1 g z + \rho_1 g(H_1+\eta) + P_S, \\ p_2 &= -\rho_2 g z + g(\rho_2 - \rho_1)\xi + \rho_1 g(H_1+\eta) + P_S. \end{aligned}\right\} \tag{4.1.1}$$

We average the motion in the upper and lower layer:

$$(\hat{u}_1, \hat{v}_1) = \frac{1}{h_1} \int_{\xi}^{H_1+\eta} (u_1, v_1)\, dz\,, \tag{4.1.2}$$

$$(\hat{u}_2, \hat{v}_2) = \frac{1}{h_2} \int_{-H_2}^{\xi} (u_2, v_2)\, dz\,, \tag{4.1.3}$$

Here, $h_1 = H_1 + \eta - \xi$ and $h_2 = \xi + H_2$ are the total depths of the upper and lower layers, respectively.

We assume that our equations can be linearized, i.e. we neglect the convective accelerations. Furthermore, we will disregard the effect of the horizontal eddy viscosity, and apply a friction force of the form (1.1.8). By introducing volume transports

$$\left.\begin{aligned}(U_1,V_1) &= h_1(\hat{u}_1,\hat{v}_1),\\ (U_2,V_2) &= h_2(\hat{u}_2,\hat{v}_2),\end{aligned}\right\} \tag{4.1.4}$$

the momentum equation for the upper layer becomes:

$$\left.\begin{aligned}U_{1t} - fV_1 &= -gh_1\eta_x - \frac{h_1}{\rho_1}P_{Sx} + \frac{1}{\rho_1}\tau_S^{(x)} - \frac{1}{\rho_1}\tau_i^{(x)},\\ V_{1t} + fU_1 &= -gh_1\eta_y - \frac{h_1}{\rho_1}P_{Sy} + \frac{1}{\rho_1}\tau_S^{(y)} - \frac{1}{\rho_1}\tau_i^{(y)}.\end{aligned}\right\} \tag{4.1.5}$$

Here ($\tau_i^{(x)}$, $\tau_i^{(y)}$) are the internal frictional stresses between the layers.

Equivalently, for the lower layer we find

$$\left.\begin{aligned}U_{2t} - fV_2 &= -\frac{\rho_1}{\rho_2}gh_2\eta_x - g_*h_2\xi_x - \frac{h_2}{\rho_2}P_{Sx} + \frac{1}{\rho_2}\tau_i^{(x)} - \frac{1}{\rho_2}\tau_B^{(x)},\\ V_{2t} + fU_2 &= -\frac{\rho_1}{\rho_2}gh_2\eta_y - g_*h_2\xi_y - \frac{h_2}{\rho_2}P_{Sy} + \frac{1}{\rho_2}\tau_i^{(y)} - \frac{1}{\rho_2}\tau_B^{(y)},\end{aligned}\right\} \tag{4.1.6}$$

where we have defined

$$g_* \equiv \left(\frac{\rho_2 - \rho_1}{\rho_2}\right)g\,, \tag{4.1.7}$$

which is referred to as the *reduced* gravity, because the fraction $(\rho_2 - \rho_1)/\rho_2$ is small for typical ocean conditions.

By integrating the continuity equation (1.1.10) in each layer, we find, without any linearization of the boundary conditions, that

$$\left.\begin{aligned}\eta_t - \xi_t &= -U_{1x} - V_{1y},\\ \xi_t &= -U_{2x} - V_{2y}.\end{aligned}\right\} \tag{4.1.8}$$

4.2 Barotropic response

Assume that the mean velocities in each layer are approximately equal, i.e. $\hat{u}_1 \approx \hat{u}_2$, $\hat{v}_1 \approx \hat{v}_2$. This leads to

$$\frac{U_1}{H_1} \approx \frac{U_2}{H_2}, \quad \frac{V_1}{H_1} \approx \frac{V_2}{H_2}, \tag{4.2.1}$$

when we assume that $|\eta|, |\xi| << H_1, H_2$. For simplicity, we also take that the lower layer has a constant depth. From (4.1.8) we then obtain

$$\eta_t - \xi_t = -\frac{H_1}{H_2}(U_{2x} + V_{2y}) = \frac{H_1}{H_2}\xi_t, \tag{4.2.2}$$

or

$$\xi = \frac{H_2}{H_1 + H_2}\eta. \tag{4.2.3}$$

Here the integration constant must be zero when we consider wave motion. We note from (4.2.3) that ξ and η are in phase, and that $|\xi| < |\eta|$.

By neglecting the effect of the earth's rotation, assuming constant surface pressure, neglecting frictional effects, and taking $h_1 \approx H_1$ in (4.1.5), equations (4.1.8) and (4.2.3) yield

$$\eta_{tt} - g(H_1 + H_2)\eta_{xx} = 0, \tag{4.2.4}$$

when $\partial / \partial y = 0$. The solution is

$$\eta = F_1(x - c_0 t) + F_2(x + c_0 t), \tag{4.2.5}$$

where $c_0^2 = g(H_1 + H_2)$. The expression (4.2.5) describes long surface waves propagating in a non-rotating canal with depth $H_1 + H_2$. This is the solution we would have found if we, as a starting point, had neglected the density difference between the layers; see the one-layer model in Section 2.3. Such a solution (a free wave), which is not influenced by the small density difference between the layers, is often referred to as the *barotropic* response.

The original meaning of the word “barotropic” is related to the field of mass, and expresses the fact that the pressure is constant along the density surfaces, i.e. the isobaric and isopycnal surfaces coincide. Mathematically this can be expressed as $\nabla p \times \nabla \rho = 0$. This was the case for the free waves in Chapter II, where the density was constant everywhere, and the pressure was constant along the sea surface. For the two-layer model this would mean that the pressure should be constant along the interface between the two layers. This is only approximately satisfied here, but nonetheless it has become customary to denote the response in this case as the barotropic response.

4.3 Baroclinic response

We now assume that $|\eta_t| << |\xi_t|$. Then, from (4.1.8):

$$(U_1 + U_2)_x + (V_1 + V_2)_y = 0 . \tag{4.3.1}$$

For simplicity we take the bottom to be flat. A particular solution of (4.3.1) can be written

$$\left.\begin{aligned} U_1 &= -U_2, \\ V_1 &= -V_2, \end{aligned}\right\} \tag{4.3.2}$$

i.e. the volume fluxes are equal, but oppositely directed in each layer. By taking the surface pressure to be constant, and neglecting the effect friction, summation of (4.1.5) and (4.1.6) yields

$$\xi = -\left[\frac{\rho_2 H_1 + \rho_1 H_2}{(\rho_2 - \rho_1) H_2}\right]\eta , \tag{4.3.3}$$

where, as in the barotropic case, the integration constant must be zero. Furthermore, we have used that $h_1 \approx H_1$, $h_2 \approx H_2$. The difference between ρ_1 and ρ_2 is quite small,

which allows us to use the approximations $\rho_2 - \rho_1 = \Delta\rho$, and $\rho_1 \sim \rho_2 \approx \rho$. Thus, equation (4.3.3) can be rewritten as

$$\xi = -\frac{\rho}{\Delta\rho}\left[\frac{H_1 + H_2}{H_2}\right]\eta\,. \tag{4.3.4}$$

We note that ξ and η are oppositely directed, and that $|\xi| >> |\eta|$, as initially assumed.

Assuming that $\partial/\partial y = 0$, and neglecting the effects of friction and the earth's rotation, we obtain from (4.1.6) with $h_2 \approx H_2$, (4.1.8), and (4.3.3) that

$$\xi_{tt} - c_1^2 \xi_{xx} = 0\,, \tag{4.3.5}$$

where

$$c_1^2 = g_* \frac{H_1 H_2}{H_1 + H_2}\,. \tag{4.3.6}$$

Here we have assumed that $\rho_1 H_2 / \rho_2 \approx H_2$. The solution of (4.3.5) can be written

$$\xi = F_1(x - c_1 t) + F_2(x + c_1 t)\,. \tag{4.3.7}$$

This represents internal gravity waves propagating with phase speed c_1 along the interface between the layers; see the sketch in Fig. 4.2.

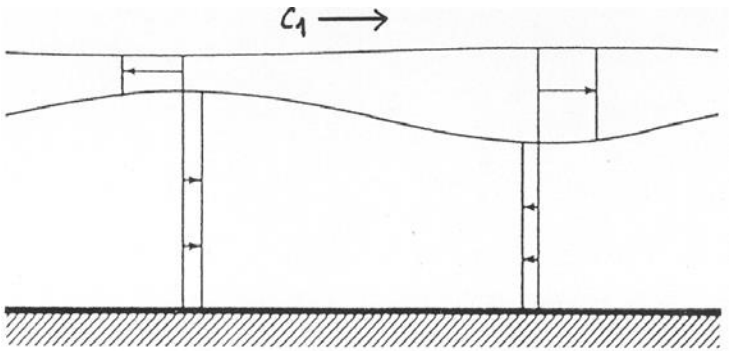

Fig. 4.2 *Internal wave in a two-layer model.*

The solution to (4.3.7) is often called the *baroclinic* response. As for barotropic, the term "baroclinic" is linked to the mass field. In a baroclinic mass field the constant pressure surfaces and the constant density surfaces intersect, i.e. $\nabla p \times \nabla \rho \neq 0$.

Equation (4.3.4) shows that this is the case here, since, when $\xi > 0$, then $\eta < 0$. Accordingly, the pressure varies along the interface, which is a constant density surface.

Let us assume that the lower layer is very deep, i.e. $H_2 >> H_1$. This is the most common configuration in the ocean. From (4.1.6) we find for the *x*-component in the lower layer

$$\frac{\rho_1}{\rho_2} g\eta_x = -g_*\xi_x - \frac{1}{\rho_2} P_{Sx} + \frac{1}{h_2}\left[\frac{1}{\rho_2}\tau_i^{(x)} - \frac{1}{\rho_2}\tau_B^{(x)} - U_{2t} + fV_2\right]. \qquad (4.3.8)$$

For the baroclinic case, U_2 and V_2 are finite when $h_2 \to \infty$, and so are the frictional stresses. Accordingly, for this limit, (4.3.8) reduces to

$$g\eta_x = -\frac{\rho_2}{\rho_1} g_*\xi_x - \frac{1}{\rho_1} P_{Sx}. \qquad (4.3.9)$$

In the same way we find for the *y*-component:

$$g\eta_y = -\frac{\rho_2}{\rho_1} g_*\xi_y - \frac{1}{\rho_1} P_{Sy}. \qquad (4.3.10)$$

By inserting (4.3.9) and (4.3.10) into (4.1.5) for the upper layer, we find that

$$\left.\begin{aligned} U_{1t} - fV_1 &= \frac{\rho_2}{\rho_1} h_1 g_*\xi_x + \frac{1}{\rho_1}\tau_S^{(x)} - \frac{1}{\rho_1}\tau_i^{(x)}, \\ V_{1t} + fU_1 &= \frac{\rho_2}{\rho_1} h_1 g_*\xi_y + \frac{1}{\rho_1}\tau_S^{(y)} - \frac{1}{\rho_1}\tau_i^{(y)}. \end{aligned}\right\} \qquad (4.3.11)$$

For the baroclinic case, the depth of the upper layer can be written $h_1 = H_1 - \xi + \eta \approx H_1 - \xi$. Furthermore, we apply that $\rho_2 - \rho_1 = \Delta\rho$, and $\rho_1 \approx \rho_2 = \rho$. By linearizing the pressure term (the first term on the right-hand side), equations (4.1.8) and (4.3.11) yield

$$\left.\begin{aligned} U_{1t} - fV_1 &= -g_* H_1 h_{1x} + \frac{1}{\rho}\tau_S^{(x)} - \frac{1}{\rho}\tau_i^{(x)}, \\ V_{1t} + fU_1 &= -g_* H_1 h_{1y} + \frac{1}{\rho}\tau_S^{(y)} - \frac{1}{\rho}\tau_i^{(y)}, \\ h_{1t} &= -U_{1x} - V_{1y}. \end{aligned}\right\} \qquad (4.3.12)$$

These equations for the baroclinic response in the upper layer are formally identical to the equations describing the storm surge problem for a quasi-homogeneous ocean; see (1.5.2), when the upper layer thickness replaces the surface elevation, and the gravity g is replaced by g_*. The set of equations (4.3.12) describes what is often referred to as a *reduced* gravity model for the volume transport in the upper layer. Even though the numerical values for the volume fluxes in the lower layer are of the same order of magnitude as in the upper layer, the *mean velocity* in the lower layer is negligible, since $H_2 \to \infty$. Therefore, we usually say that the lower layer has no motion in this approximation.

We immediately realize from (4.3.12) that transient phenomena such as Sverdrup-, Kelvin- and planetary Rossby waves in a rotating ocean of constant density have their internal (baroclinic) counter-parts in a two-layer model. The analysis for the internal response is identical to the analysis in Chapter III. It often suffices to replace g with g_* and H with H_1 in the solution for the barotropic response.

Analogous to the barotropic case we can define a length scale a_1 that characterizes the significance of earth's rotation. We write

$$a_1 = c_1 / f\ , \qquad (4.3.13)$$

where $c_1^2 = g_* H_1$. The length scale a_1 is called the internal, or baroclinic, Rossby radius. Typical values for c_1 in the ocean are 2-3 m s^{-1}. Hence, $a_1 \approx$ 20-30 km, which is much less than the typical barotropic Rossby radius. Therefore, the effect of earth's

rotation will be much more important for the baroclinic response than for the barotropic one with the same horizontal scale, or wavelength.

4.4 Continuously stratified fluid

We now turn to the more general problem of continuous density stratification, and start by investigating the stability of a stratified incompressible fluid under the influence of gravity. The equilibrium values are:

$$\left.\begin{aligned} &\vec{v} = 0, \\ &\rho = \rho_0(z), \\ &p = p_0(z) = -g\int \rho_0\, dz + \text{const.} \end{aligned}\right\} \tag{4.4.1}$$

We introduce small perturbations (denoted by primes) from the state of equilibrium, writing the velocity, density, and pressure as

$$\left.\begin{aligned} &\vec{v} = \vec{v}'(x,y,z,t), \\ &\rho = \rho_0(z) + \rho'(x,y,z,t), \\ &p = p_0(z) + p'(x,y,z,t). \end{aligned}\right\} \tag{4.4.2}$$

We assume that the density is conserved for a fluid particle. Furthermore, we take that the perturbations are so small that we can linearize our problem, i.e. neglect terms that contain products of perturbation quantities. Using a horizontal friction force of the type (1.1.8), the equations for the conservation of momentum, density, and mass then reduce to

$$\rho_0(z)(u_t - fv) = -p_x + \tau_z^{(x)}, \tag{4.4.3}$$

$$\rho_0(z)(v_t + fu) = -p_y + \tau_z^{(y)}, \tag{4.4.4}$$

$$\rho_0(z)w_t = -p_z - \rho g, \tag{4.4.5}$$

$$\rho_t + \frac{d\rho_0}{dz}w = 0, \tag{4.4.6}$$

$$u_x + v_y + w_z = 0. \tag{4.4.7}$$

Here we have for simplicity left out the primes that mark the perturbations. Furthermore, we have neglected the effect of friction in vertical component of the momentum equation (4.4.5).

4.5 Free internal waves in a rotating ocean

We start by disregarding completely the effect of friction on the fluid motion, i.e. we take $\tau^{(x)} = \tau^{(y)} = 0$ in (4.4.3) and (4.4.4). Furthermore, we introduce the Brunt-Väisälä frequency (or the buoyancy frequency) *N*, defined by

$$N^2(z) = -\frac{g}{\rho_0}\frac{d\rho_0}{dz}. \tag{4.5.1}$$

We are here going to study motion in a stably stratified incompressible fluid. In this case we must have that $d\rho_0 / dz < 0$, meaning that *N* is real and positive. Equation (4.4.6) can then be written

$$g\rho_t - N^2\rho_0 w = 0. \tag{4.5.2}$$

By differentiating (4.4.5) with respect to time, and utilizing (4.5.2), we find that

$$\rho_0(w_{tt} + N^2 w) = -p_{zt}. \tag{4.5.3}$$

From this equation we note that the time scale for pure vertical motion ($p_{zt} = 0$) is N^{-1}. Elimination of the pressure gradient from (4.4.3)-(4.4.4), yields the vorticity equation. On an *f*-plane we obtain

$$(v_x - u_y)_t = fw_z, \tag{4.5.4}$$

where we have applied (4.4.7). Forming the horizontal divergence from the same two equations, we find

$$\rho_0(z)\{w_{zt} + f(v_x - u_y)\} = \nabla_H^2 p. \tag{4.5.5}$$

Elimination of the vorticity from the equations above, yields

$$\rho_0\left[w_{ztt} + f^2 w_z\right] = \nabla_H^2 p_t . \tag{4.5.6}$$

Finally, by eliminating the pressure between (4.5.3) and (4.5.6), we obtain

$$\left[\nabla_H^2 w + \frac{1}{\rho_0}(\rho_0 w_z)_z\right]_{tt} + N^2\nabla_H^2 w + f^2\frac{1}{\rho_0}(\rho_0 w_z)_z = 0 , \tag{4.5.7}$$

where $\nabla_H^2 \equiv \partial^2/\partial x^2 + \partial^2/\partial y^2$. We simplify (4.5.7) by assuming that $\rho_0(z)$ varies *slowly* over the typical vertical scale for *w*, i.e.

$$\frac{1}{\rho_0}(\rho_0 w_z)_z \approx w_{zz} . \tag{4.5.8}$$

This is *Boussinesq approximation* for internal waves. By introducing the Brunt-Väisälä frequency (4.5.1), we can write

$$\frac{1}{\rho_0}(\rho_0 w_z)_z = -\frac{N^2}{g} w_z + w_{zz} . \tag{4.5.9}$$

We realize from (4.5.8) that the Boussinesq approximation implies that

$$\left|\frac{N^2}{g} w_z\right| << \left|w_{zz}\right| . \tag{4.5.10}$$

If *d* is a typical vertical scale for the motion, the above equation yields

$$N^2 << g/d , \tag{4.5.11}$$

where $d_{\max} \le H$. For a shallow ocean we typically have that $g/H \sim 10^{-1}\,\mathrm{s}^{-2}$, while for a deep ocean (H = 4000 m), the corresponding value becomes $g/H \sim \frac{1}{4}\times 10^{-2}\,\mathrm{s}^{-2}$. Measurements in the ocean show that $N^2 \sim 10^{-4} - 10^{-6}\,\mathrm{s}^{-2}$, so (4.5.11) is usually very well satisfied. We will therefore utilize the Boussinesq approximation in the future analysis of this problem. Equation (4.5.7) then reduces to

$$\nabla^2 w_{tt} + N^2(z)\nabla_H^2 w + f^2 w_{zz} = 0 . \tag{4.5.12}$$

We derive the same equation by letting $\rho_0(z) \approx \rho_r$ on the left-hand sides of (4.4.3)-(4.4.5), where ρ_r is a constant reference density. Then, $N^2 = -(g/\rho_r)d\rho_0/dz$. This latter approach is probably the most common one when applying the Boussinesq approximation.

We assume that the ocean is unlimited in the horizontal direction, and consider a wave solution of the form

$$w = W(z)\exp(i(kx - \omega t)). \tag{4.5.13}$$

Here the *x*-axis is directed along the wave propagation direction. From (4.5.12) we then obtain

$$W'' + k^2\left[\frac{N^2 - \omega^2}{\omega^2 - f^2}\right]W = 0, \tag{4.5.14}$$

where a prime denote differentiation with respect to *z*.

4.6 Constant Brunt-Väisälä frequency

Later on we shall allow *N* to vary with *z*. In this section, we simplify, and assume that *N* is constant. Typical values for *N* and *f* in the ocean (and atmosphere) are $N \sim 10^{-2}$ s^{-1} and $f \sim 10^{-4}$ s^{-1}, i.e. $N >> f$. From equation (4.5.14) we then note that we have wave solutions in the *z*-direction if $f < \omega < N$, while for $\omega < f$ or $\omega > N$, the solutions must be of exponential character in the *z*-direction.

Let us assume that $f < \omega < N$. We then take

$$W \propto \exp(imz), \tag{4.6.1}$$

where *m* is a real wave number in the vertical direction. By insertion into (4.5.14), we obtain the dispersion relation

$$\omega^2 = \frac{k^2N^2 + m^2f^2}{k^2 + m^2}. \tag{4.6.2}$$

From the discussion in Section 2.7 we realize that we have anisotropic system, since ω cannot be expressed solely as a function of the magnitude of the wave number vector.

We can nowdefine a wave number vector as

$$\vec{\kappa} = (k, m)\,. \tag{4.6.3}$$

Then the phase speed and group velocity, become, respectively

$$\vec{c} = \omega\vec{\kappa}/\kappa^2\,, \tag{4.6.4}$$

and

$$\vec{c}_g = \nabla_\kappa \omega\,. \tag{4.6.5}$$

When ω is constant, (4.6.2) yields that the isolines are straight lines through the origin in wave number space. Along the *m*-axis (where $k = 0$), we have $\omega = f$ (small). Along the *k*-axis (where $m = 0$), we have $\omega = N$ (large). Since, from (4.6.5), the group velocity is always directed towards increasing values of ω, while the phase speed (4.6.4) is directed along the wave number vector, we may sketch the direction of the phase speed and the group velocity as in Fig. 4.3.

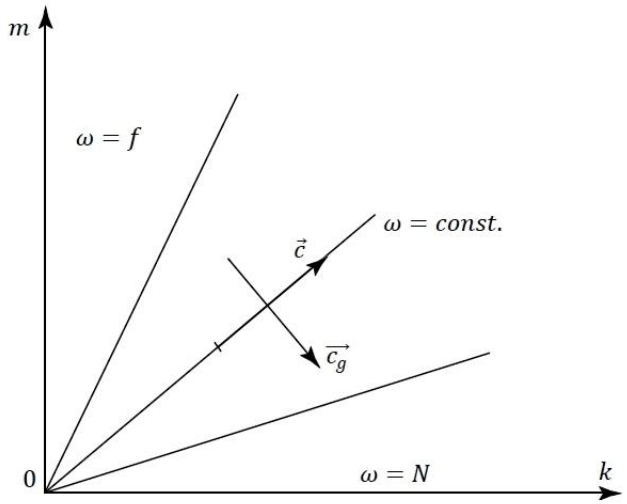

Fig. 4.3 *Lines of constant frequency for internal waves with rotation in the two-dimensional wave number space.*

If we imagine that the wave number *m* is *given*, we can plot ω as a function of *k*, as depicted in Fig. 4.4.

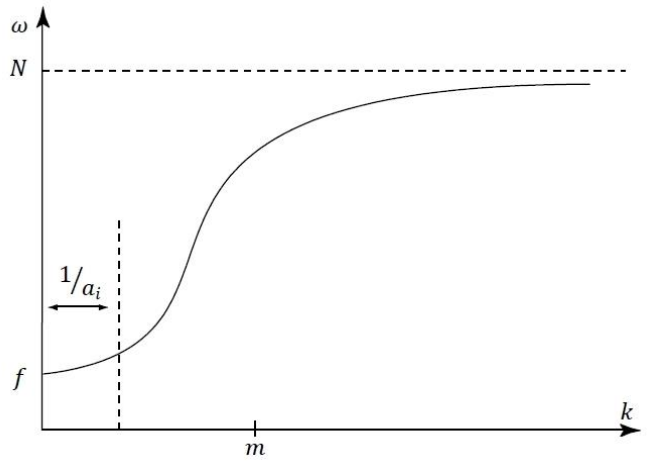

Fig. 4.4 *Dispersion diagram for internal waves with rotation.*

We can define a Rossby radius of deformation for internal motion with vertical wave number *m* by

$$a_i = \frac{N}{mf}. \tag{4.6.6}$$

For $k << a_i^{-1}$, the effect of rotation dominates (compare with Fig. 3.2 for the barotropic case).

In the ocean, the wave number *m* cannot be chosen arbitrarily, since the vertical distance is limited by the depth. If we, for simplicity, disregard the surface elevation and assume a constant depth, we must have that $w = 0$ for $z = 0, H$; see Fig. 4.5.

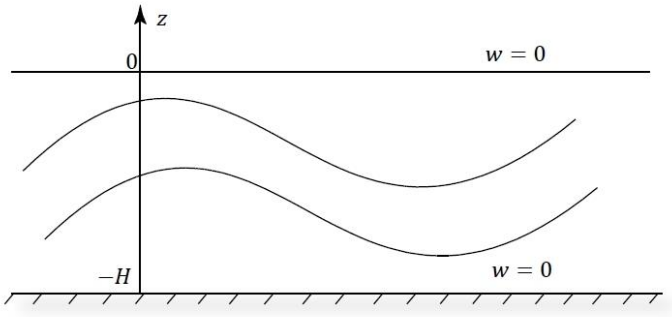

Fig. 4.5 *Internal waves in an ocean with horizontal surface and horizontal bottom.*

A solution of (4.5.14), which satisfies the upper boundary condition, is

$$W = C\sin mz\,, \tag{4.6.7}$$

where

$$m^2 = k^2\left[\frac{N^2-\omega^2}{\omega^2-f^2}\right]. \tag{4.6.8}$$

For the solution to satisfy the boundary condition at $z=-H$, we must require

$$m=\frac{n\pi}{H}, \qquad n=1,\,2,\,... \tag{4.6.8}$$

This means that vertical wave number must form a discrete (but infinite) set. Equation (4.6.8) then yields for the frequency

$$\omega=\left[\frac{k^2N^2+f^2n^2\pi^2/H^2}{k^2+n^2\pi^2/H^2}\right]^{1/2}. \tag{4.6.9}$$

We see that, for a disturbance with a *given* wave number *k* in the horizontal direction, the system (ocean) responds with a discrete number of eigenfrequencies (4.6.9).

The solution for *w* in this case can be written

$$\begin{aligned} w &= C\sin(mz)\exp\{i(kx-\omega t)\} \\ &= \frac{C}{2i}\left(\exp\{i(kx+mz-\omega t)\}-\exp\{i(kx-mz-\omega t)\}\right). \end{aligned} \tag{4.6.10}$$

The latter expression can be interpreted as the superposition of waves in a horizontal layer consisting of an incoming, obliquely upward propagating wave, and an obliquely downward reflected wave, where *m* must attain the value (4.6.8) for the wave system to satisfy the boundary condition at the bottom.

We now consider the case where the motion is mainly horizontal. This allows us to disregard the vertical acceleration in the momentum equation, i.e. we apply the hydrostatic approximation. Accordingly, in (4.5.3) we take that

$$\left|w_{tt}\right| << \left|N^2 w\right|, \tag{4.6.11}$$

which leads to

$$N^2 w \approx -\frac{1}{\rho_0} p_{zt}. \tag{4.6.12}$$

From (4.6.11) we realize that the hydrostatic approximation implies that

$$\omega^2 << N^2. \tag{4.6.13}$$

From Fig. 4.4 we note that this requires that $k << m$, i.e. the horizontal scale of motion is much larger than the vertical scale. Since the depth *H* yields the upper limit for the vertical scale, disturbances with wavelength $\lambda >> H$ will satisfy the hydrostatic condition. This requirement applies to barotropic surface waves as well as baroclinic internal waves.

Applying the hydrostatic approximation, (4.6.2) reduces to

$$\omega = \left[f^2 + \frac{k^2 N^2}{m^2} \right]^{1/2}. \tag{4.6.14}$$

This is the frequency for *internal* Sverdrup waves. For an ocean with depth *H* and a horizontal surface, i.e. $m = n\pi / H$ as in equation (4.6.8), we can write

$$\omega = (f^2 + c_n^2 k^2)^{1/2}. \tag{4.6.15}$$

Here

$$c_n = HN/(n\pi), \quad n = 1, 2, 3, ... \tag{4.6.16}$$

which is the phase speed for long internal waves in the non-rotating case. Since

$$m = n\pi / H = N / c_n , \tag{4.6.17}$$

equation (4.6.6) yields the internal (baroclinic) Rossby radius

$$a_i = a_n = c_n / f , \quad n = 1, 2, 3, ... \tag{4.6.18}$$

We note that this is analogous to the definition of the barotropic Rossby radius appearing in (3.2.4). For one single internal mode, i.e. a two-layer structure, this is similar to (4.3.13).

4.7 Internal response to wind forcing; upwelling at a straight coast

We apply the set of equations (4.4.3)-(4.4.7), and utilize the Boussinesq approximation and the hydrostatic approximation, i.e.

$$\left.\begin{aligned} u_t - fv &= -\frac{1}{\rho_r} p_x + \frac{1}{\rho_r} \tau_z^{(x)}, \\ v_t + fu &= -\frac{1}{\rho_r} p_y + \frac{1}{\rho_r} \tau_z^{(y)}, \end{aligned}\right\} \tag{4.7.1}$$

$$p_z = -\rho g . \tag{4.7.2}$$

Furthermore, we introduce the vertical displacement $\xi(x, y, z, t)$ of a material surface, so that $w = D\xi / dt$ in the fluid. Linearly, this becomes

$$w = \xi_t . \tag{4.7.3}$$

The conservation of density (4.4.6) then yields for the density perturbation

$$\rho = \frac{\rho_r}{g} N^2 \xi . \tag{4.7.4}$$

where we have assumed that $\rho = \xi = 0$ at $t = 0$. Inserting into (4.7.2), we obtain

$$p_z = -\rho_r N^2 \xi , \tag{4.7.5}$$

while the continuity equation can be written

$$\xi_{zt} = -u_x - v_y \,. \tag{4.7.6}$$

In general, we take that $N = N(z)$, and we write the solutions to our problem as infinite series. For simplicity, we assume that the depth is constant, and that the surface is horizontal at all times. Accordingly:

$$\xi = 0, \quad z = -H, 0. \tag{4.7.7}$$

In principle, it is also possible to allow the position of the surface to vary in time and space. However, the solution shows that the *internal* response can be achieved, to a good approximation, by assuming a horizontal surface (the rigid lid approximation); see Gill and Clark (1974). According to our adopted approach, we write the solutions as

$$\left.\begin{aligned} u &= \sum_{n=1}^{\infty} u_n(x,y,t)\ \phi_n'(z), \\ v &= \sum_{n=1}^{\infty} v_n(x,y,t)\ \phi_n'(z), \\ p &= \rho_r \sum_{n=1}^{\infty} p_n(x,y,t)\ \phi_n'(z), \\ \xi &= \sum_{n=1}^{\infty} \xi_n(x,y,t)\ \phi_n(z), \end{aligned}\right\} \tag{4.7.8}$$

where the primes denote differentiation with respect to *z*. By inserting the solutions into (4.7.5), we find

$$\sum_{n=1}^{\infty} p_n(x,y,t)\left[\phi_n''(z) + \frac{\xi_n}{p_n} N^2 \phi_n(z)\right] = 0 \,. \tag{4.7.9}$$

For the variables to separate, we must require

$$\frac{\xi_n}{p_n} = \text{const.} = \frac{1}{c_n^2} \,. \tag{4.7.10}$$

Furthermore, for (4.7.9) to be satisfied for all *x*, *y* and *t*, we must have that

$$\phi_n'' + \frac{N^2}{c_n^2}\phi_n = 0\,. \tag{4.7.11}$$

The boundary conditions (4.7.7) yield

$$\phi_n = 0, \quad z = -H, 0\,. \tag{4.7.12}$$

Equation (4.7.11) and the boundary conditions (4.7.12) define an *eigenvalue* problem, i.e. for given $N = N(z)$ we can, in principle, determine the constant *eigenvalues* c_n, and the *eigenfunctions* $\phi_n(z)$, which appear in the series (4.7.8).

It is easy to demonstrate that the differentiated eigenfunctions ϕ_n' constitute an orthogonal set. Since (4.7.11) is valid for arbitrary numbers *n* and *m*, we can write

$$\left.\begin{aligned} c_n^2\phi_n'' + N^2\phi_n = 0, \\ c_m^2\phi_m'' + N^2\phi_m = 0, \end{aligned}\right\} \tag{4.7.13}$$

where $m \neq n$. We multiply the upper and lower equations by ϕ_m and ϕ_n, respectively. By subtracting and integrating from $z = -H$ to $z = 0$, utilizing (4.7.12), we find

$$(c_n^2 - c_m^2)\int_{-H}^{0} \phi_n'\phi_m'\,dz = 0\,. \tag{4.7.14}$$

Accordingly, for $n \neq m$, i.e. $c_n \neq c_m$, we must have that

$$\int_{-\mathrm{H}}^{0} \phi_n'\phi_m'\,dz = 0, \quad n \neq m\,, \tag{4.7.15}$$

which proves the orthogonality. Since the eigenfunctions are known, apart from multiplying constants (as for all homogeneous problems), we can normalize them by assuming, for example, that

$$\int_{-H}^{0} \phi_n'^2\,dz = \frac{H}{2}\,. \tag{4.7.16}$$

This procedure is generally valid for $N = N(z)$. To exemplify, and discuss explicit solutions in a simple way, we assume that *N* is constant. Then the eigenfunctions become

$$\phi_n = A_n \sin\left(\frac{N}{c_n} z\right), \tag{4.7.17}$$

which satisfies equation (4.7.11) and the upper boundary condition. The requirement $\phi_n(-H) = 0$ yields the eigenvalues:

$$\frac{HN}{c_n} = n\pi, \tag{4.7.18}$$

or $c_n = HN/(n\pi)$, which is identical to (4.6.16). Finally, the normalization condition (4.7.15) gives $A_n = H/(n\pi)$.

We now insert the series (4.7.8) into (4.7.1) and (4.7.6), and multiply each equation with ϕ_1', ϕ_2', ϕ_3', etc. By integrating from $z = -H$ to $z = 0$, and applying the orthogonality condition (4.7.15), we finally obtain

$$\left.\begin{aligned} \frac{\partial u_n}{\partial t} - f v_n &= -c_n^2 \frac{\partial \xi_n}{\partial x} + \tau_n^{(x)}, \\ \frac{\partial v_n}{\partial t} + f u_n &= -c_n^2 \frac{\partial \xi_n}{\partial y} + \tau_n^{(y)}, \\ \frac{\partial \xi_n}{\partial t} &= -\frac{\partial u_n}{\partial x} - \frac{\partial v_n}{\partial y}, \end{aligned}\right\} \tag{4.7.19}$$

where

$$\left.\begin{aligned} \tau_n^{(x)} &= \frac{2}{\rho_r H} \int_{-H}^{0} \frac{\partial \tau^{(x)}}{\partial z} \phi_n' \, dz, \\ \tau_n^{(y)} &= \frac{2}{\rho_r H} \int_{-H}^{0} \frac{\partial \tau^{(y)}}{\partial z} \phi_n' \, dz. \end{aligned}\right\} \tag{4.7.20}$$

We notice from (4.7.19) that this set of equations is formally identical to the equations for the barotropic volume transports driven by surface winds, e.g. (1.5.2).

The horizontal shear stress gradients $\tau_z^{(x)}$ and $\tau_z^{(y)}$ appear in (4.7.20). In principle, these are unknown, and depend on the fluid motion. However, we shall simplify the problem by assuming that we can assess these gradients in the fluid.

Assume that a constant wind is blowing along a straight coast, so that the surface wind stresses become $\tau_S^{(x)} \neq 0$, $\tau_S^{(y)} = 0$; see the sketch in Fig. 4.6. The model is situated in the northern hemisphere, i.e. $f > 0$.

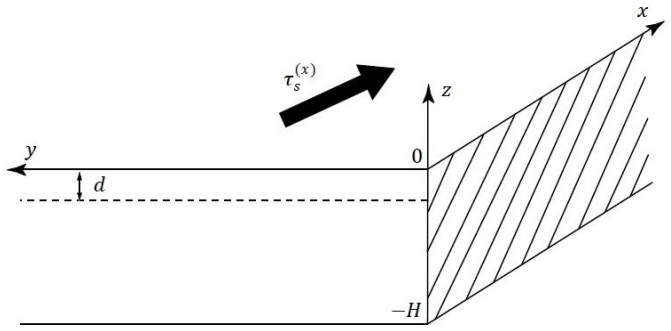

Fig. 4.6 *Model sketch of upwelling/downwelling at a straight coast*.

We assume that the shear stresses are only felt in a relatively thin layer close to the surface, i.e. the mixed layer, with a thickness $d << H$. Here the stresses vary linearly with depth:

$$\left.\begin{aligned} \tau^{(x)} &= \begin{cases} \tau_S^{(x)}\left(\dfrac{z+d}{d}\right), & -d \le z \le 0, \\ 0, & -H \le z \le -d, \end{cases} \\ \tau^{(y)} &= 0, \qquad\qquad -H \le z \le 0. \end{aligned}\right\} \tag{4.7.21}$$

With this variation in *z*, (4.7.20) yields

$$\left.\begin{aligned} \tau_n^{(x)} &= -\frac{2\tau_S^{(x)}}{\rho_r H d}\phi_n(-d), \\ \tau_n^{(y)} &= 0. \end{aligned}\right\} \tag{4.7.22}$$

We assume that the solutions are independent of the along-shore coordinate *x*, i.e., from (4.7.19):

$$\left.\begin{aligned} \frac{\partial u_n}{\partial t} - f v_n &= \tau_n^{(x)}, \\ \frac{\partial v_n}{\partial t} + f u_n &= -c_n^2 \frac{\partial \xi_n}{\partial y}, \\ \frac{\partial \xi_n}{\partial t} &= -\frac{\partial v_n}{\partial y}. \end{aligned}\right\} \tag{4.7.23}$$

These equations have a particular solution where v_n is independent of time. By assuming that $\partial v_n / \partial t = 0$, and eliminating u_n, ξ_n from the equations above, we find

$$\frac{\partial^2 v_n}{\partial y^2} - \frac{1}{a_n^2} v_n = \frac{f}{c_n^2} \tau_n^{(x)}, \tag{4.7.24}$$

where $a_n = c_n / f$ is the Rossby radius for internal waves. By requiring that

$$\left.\begin{aligned} v_n &= 0, \quad y = 0, \\ v_n &\text{ finite}, \; y \to \infty, \end{aligned}\right\} \tag{4.7.25}$$

the solution of (4.7.25) becomes

$$v_n = -\frac{\tau_n^{(x)}}{f}\left(1 - \exp(-y / a_n)\right). \tag{4.7.26}$$

From (4.7.23) we then obtain

$$\left.\begin{aligned} u_n &= \tau_n^{(x)} t \, \exp(-y / a_n), \\ \xi_n &= \frac{\tau_n^{(x)} t}{f a_n} \exp(-y / a_n). \end{aligned}\right\} \tag{4.7.27}$$

Thus, u_n and ξ_n increase *linearly* in time during the action of the wind. From the derived solution we see that a wind parallel to the coast results in upwelling or downwelling within an area limited by the coast and the baroclinic Rossby radius. Within this area we also notice the presence of a jet-like flow u_n parallel to the coast.

This flow is geostrophically balanced; see the second equation in (4.7.23) with $\partial v_n / \partial t = 0$.

We now discuss our solution in some more details. For this purpose the first term in the series (4.7.8) for *v* and ξ suffices:

$$\left.\begin{aligned} v &= v_1 \phi_1'(z) + \ldots \\ \xi &= \xi_1 \phi_1(z) + \ldots \end{aligned}\right\} \tag{4.7.28}$$

To simplify, we again take that *N* is constant. Then, from (4.7.17), (4.7.18) and (4.7.22):

$$\left.\begin{aligned} \phi_1 &= \frac{H}{\pi}\sin\left(\frac{\pi z}{H}\right), \\ c_1 &= HN/\pi, \\ \tau_1^{(x)} &= \frac{2\tau_S^{(x)}}{\rho_r \pi d}\sin\left(\frac{\pi d}{H}\right). \end{aligned}\right\} \tag{4.7.29}$$

By inserting into (4.7.28), we find

$$\left.\begin{aligned} v &= -\frac{2\tau_S^{(x)}}{\pi \rho_r f d}\sin\left(\frac{\pi d}{H}\right)\left(1-\exp(-y/a_1)\right)\cos\left(\frac{\pi z}{H}\right) + \ldots \\ w &= \xi_t = \frac{2\tau_S^{(x)}}{\pi \rho_r N d}\sin\left(\frac{\pi d}{H}\right)\exp(-y/a_1)\sin\left(\frac{\pi z}{H}\right) + \ldots\ldots \end{aligned}\right\} \tag{4.7.30}$$

Here $-H \le z \le 0$ and $f > 0$. For wind in the negative *x*-direction ($\tau_S^{(x)} < 0$), we find that $w \ge 0$ in the region limited by baroclinic Rossby radius. Accordingly, the Ekman surface-layer transport away from the coast leads to a compensating flow from below (upwelling). This is consistent with the sign of *v* in (4.7.30), since *v* is positive close to the surface and negative near the bottom; see the sketch in Fig. 4.7.

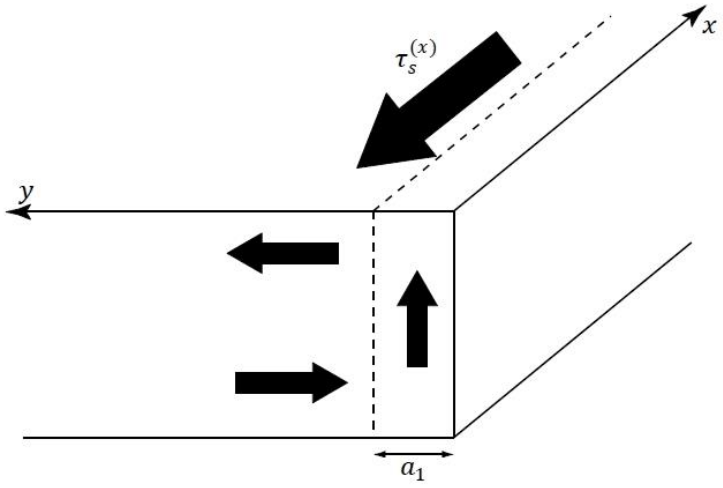

Fig. 4.7 *Sketch of an upwelling situation.*

We finally mention that since the *x*-component *u* and the vertical displacement ξ increase linearly in time, the theory developed here is only valid as long as the nonlinear terms in the equations remain small.

We return for a moment to the two-layer reduced gravity model to find out what this would yield under similar conditions. By assuming $\tau_i^{(x)} = \tau_i^{(y)} = \tau_S^{(y)} = V_{1t} = 0$ in (4.3.12), we find, analogous to (4.7.24):

$$V_{1yy} - \frac{1}{a_1^2} V_1 = \frac{f \tau_S^{(x)}}{\rho c_1^2}, \tag{4.7.31}$$

when we take that $\partial / \partial x = 0$. The solution becomes

$$\left.\begin{aligned} V_1 &= -\frac{\tau_S^{(x)}}{\rho f}\left(1 - \exp(-y/a_1)\right), \\ U_1 &= \frac{\tau_S^{(x)}}{\rho} t \exp(-y/a_1), \\ h_1 &= \frac{\tau_S^{(x)}}{\rho c_1} t \exp(-y/a_1), \end{aligned}\right\} \tag{4.7.32}$$

where $c_1 = (g_* H_1)^{1/2}$ and $a_1 = c_1 / f$. We may define an upwelling velocity, when $\tau_S^{(x)} < 0$, as

$$w_1 = -h_{1t} = -\frac{\tau_S^{(x)}}{\rho c_1}\exp(-y/a_1)\,. \qquad (4.7.33)$$

We can now compare with the case of continuous stratification. First, we assume that the layer of frictional influence is thin, i.e. $d << H$. Furthermore, we insert for $z = -H/2$ to obtain the maximum vertical velocity. From (4.7.30) we then obtain

$$w(z = -H/2) = -\frac{2\tau_S^{(x)}}{\pi \rho_r c_1}\exp(-y/a_1)\,. \qquad (4.7.34)$$

Here $c_1 = HN/\pi$ from (4.7.29). By comparing with (4.7.33), we see that the upwelling velocities are remarkably similar, even though (4.7.34) is obtained from the first term in a series expansion.

We will not go into further details of this problem. However, it is appropriate to emphasize that this phenomenon is important for marine life. The water that upwells is coming from depths below the mixed layer, and is rich in nutrients. Hence, the upwelling process brings colder, nutrient-rich water to the euphotic zone, where there is sufficient light to support growth and reproduction of plant algae (phytoplankton). This means that upwelling areas are rich in biologic activity. Some of the world's largest catches of fish are made in such areas, e.g. off the coasts of Peru and Chile.

V. WAVE-INDUCED MASS TRANSPORT

5.1 The Stokes drift

The result in Section 2.1 that the particles in deep water waves move in closed circles is correct in the present linear approach (remember we have linearized our equations). In reality, if we do our calculations without linearization, we find that that the individual fluid particles have a slow net drift in the wave propagation direction. This is because the velocity of the fluid particle is a little larger when it is closest to the surface, than when it is farthest away from it. Hence, it moves a little more forward

than it moves backward. The resulting motion will be a forward spiral; see the sketch below.

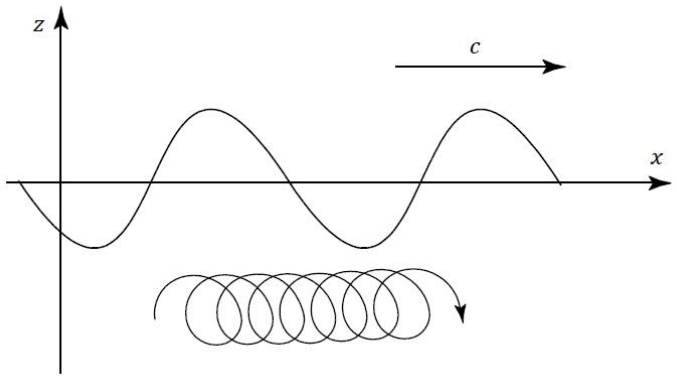

Fig. 5.1 *Sketch of nonlinear motion of a fluid particle due to waves.*

The net particle motion in this case can be obtained by considering the *Lagrangian* velocity, which is the velocity of an individual fluid particle. We denote it by $\vec{v}_L$. Then $\vec{v}_L(\vec{r}_0,t)$ is the velocity of a fluid particle whose position at time $t=t_0$ is $\vec{r}_0=(x_0,y_0,z_0)$. At a later time *t*, the particle has moved to a new position

$$\vec{r}_L=\vec{r}_0+D\vec{r}\,. \tag{5.1.1}$$

where

$$D\vec{r}=\int_{t_0}^{t}\vec{v}_L(\vec{r}_0,t')dt'\,. \tag{5.1.2}$$

In our former Eulerian specification the fluid velocity at time *t* is $\vec{v}(\vec{r}_L,t)$. Hence

$$\vec{v}_L(\vec{r}_0,t)=\vec{v}(\vec{r}_L,t)\,. \tag{5.1.3}$$

By inserting for $\vec{r}_L$ from (5.1.1), we obtain

$$\vec{v}_L(\vec{r}_0,t)=\vec{v}\left(\vec{r}_0+D\vec{r},t\right). \tag{5.1.4}$$

We assume that the distance $D\vec{r}=\vec{r}_L-\vec{r}_0$ travelled by the particle in the time interval $t-t_0$ is small. Hence, from the two first terms of a Taylor series expansion we obtain

$$\vec{v}_L(\vec{r}_0,t) = \vec{v}(\vec{r}_0,t) + \frac{\partial \vec{v}}{\partial x_0} Dx + \frac{\partial \vec{v}}{\partial y_0} Dy + \frac{\partial \vec{v}}{\partial z_0} Dz = \vec{v}(\vec{r}_0,t) + D\vec{r} \cdot \nabla_L \vec{v}\,, \tag{5.1.5}$$

where $\nabla_L \equiv \vec{i}\,\partial/\partial x_0 + \vec{j}\partial/\partial y_0 + \vec{k}\partial/\partial z_0$. If we use (5.1.2), we can write (5.1.5) as

$$\vec{v}_L(\vec{r}_0,t) = \vec{v}(\vec{r}_0,t) + \left(\int_{t_0}^{t} \vec{v}_L(\vec{r}_0,t')dt' \right) \cdot \nabla_L \vec{v}(\vec{r}_0,t)\,. \tag{5.1.6}$$

The last part of the velocity on the right-hand side of (5.1.6) is called the *Stokes* velocity $\vec{v}_S$, while the first term $\vec{v}(\vec{r}_0,t)$ is the traditional Eulerian velocity. Hence, in general

$$\vec{v}_L = \vec{v} + \vec{v}_S\,. \tag{5.1.7}$$

For waves with small wave steepness the difference between $\vec{v}_L$ and $\vec{v}_E$ is small, so to second order in wave steepness we can replace the Lagrangian velocity by the Eulerian velocity in the integral of (5.1.6), i.e.

$$\vec{v}_S = \left(\int_{t_0}^{t} \vec{v}(\vec{r}_0,t')dt' \right) \cdot \nabla_L \vec{v}(\vec{r}_0,t)\,. \tag{5.1.8}$$

For waves with period *T*, the averaged Stokes velocity (denoted by an over-bar) becomes

$$\bar{\vec{v}}_S = \frac{1}{T}\int_0^T \vec{v}_S dt\,. \tag{5.1.9}$$

The averaged Stokes velocity (5.1.9) is often termed the *Stokes drift*, and constitutes a mean current induced by the waves. The Stokes drift components can be written

$$\begin{aligned}
\bar{u}_S &= \frac{1}{T}\int_0^T \left((\int_{t_0}^{t} u dt') \frac{\partial u}{\partial x_0} + (\int_{t_0}^{t} v dt') \frac{\partial u}{\partial y_0} + (\int_{t_0}^{t} w dt') \frac{\partial u}{\partial z_0} \right) dt, \\
\bar{v}_S &= \frac{1}{T}\int_0^T \left((\int_{t_0}^{t} u dt') \frac{\partial v}{\partial x_0} + (\int_{t_0}^{t} v dt') \frac{\partial v}{\partial y_0} + (\int_{t_0}^{t} w dt') \frac{\partial v}{\partial z_0} \right) dt, \\
\bar{w}_S &= \frac{1}{T}\int_0^T \left((\int_{t_0}^{t} u dt') \frac{\partial w}{\partial x_0} + (\int_{t_0}^{t} v dt') \frac{\partial w}{\partial y_0} + (\int_{t_0}^{t} w dt') \frac{\partial w}{\partial z_0} \right) dt.
\end{aligned} \tag{5.1.10}$$

5.2 Application to drift in non-rotating surface waves and in Sverdrup waves

We return to the two-dimensional Eulerian wave field for high-frequency surface waves (2.1.14), where we have neglected the effect of the earth's rotation. For calculating the Stokes drift, we have

$$\begin{aligned} u &= u(x_0, z_0, t) = \frac{\omega A \cosh(k(z_0 + H))}{\sinh(kH)} \cos(kx_0 - \omega t), \\ w &= w(x_0, z_0, t) = \frac{\omega A \sinh(k(z_0 + H))}{\sinh(kH)} \sin(kx_0 - \omega t). \end{aligned} \tag{5.2.1}$$

In this problem t_0 is arbitrary, so we take $t_0 = 0$. When we average the Stokes velocity in time, we only get non-zero contributions from $\cos^2(kx_0 - \omega t), \sin^2(kx_0 - \omega t)$ in (5.1.10). It is then easily seen that the Stokes drift components become $\bar{v}_S = \bar{w}_S = 0$, and

$$\bar{u}_S = \frac{\omega k A^2}{2 \sinh^2 kH} \cosh(2k(z_0 + H)) . \tag{5.2.2}$$

We note that the non-zero component of the Stokes drift is in the wave propagation direction. Furthermore, $\bar{u}_S$ has a maximum at the surface, where $z_0 = 0$, and it decays exponentially with depth. In this approximation we can replace z_0 with the Eulerian vertical coordinate *z*.

For Sverdrup waves in the *x*-direction, e.g. (3.3.8), we can write

$$\begin{aligned} u &= \frac{A\omega}{kH} \cos(kx_0 - \omega t), \\ v &= \frac{Af}{kH} \sin(kx_0 - \omega t), \\ w &= A\omega \left(\frac{z_0 + H}{H} \right) \sin(kx_0 - \omega t). \end{aligned} \tag{5.2.3}$$

From (5.1.10) we readily obtain that $\bar{v}_S = \bar{w}_S = 0$, and

$$\bar{u}_S = \frac{cA^2}{2H^2}, \tag{5.2.4}$$

where the phase speed c is given by (3.3.3). For Sverdrup waves the Stokes drift is independent of the depth, i.e. it does not vary with the z-coordinate.

5.3 Relation between the mean wave momentum and the energy density

When we integrate the Stokes velocity (5.1.8) from the bottom to the material surface, and then average, we obtain the total horizontal mean wave momentum $(\bar{U}_S, \bar{V}_S)$ per unit density of the problem in question. To second order in wave amplitude we have

$$\bar{U}_S = \overline{\int_{-H}^{\eta} u_S dz} \approx \int_{-H}^{0} \bar{u}_S dz, \quad \bar{V}_S = \overline{\int_{-H}^{\eta} v_S dz} \approx \int_{-H}^{0} \bar{v}_S dz, \tag{5.3.1}$$

where $(\bar{u}_S, \bar{v}_S)$ are the Stokes drift components. $\bar{U}_S, \bar{V}_S$ are also called the *Stokes fluxes.*

For surface waves, we obtain from (5.2.2):

$$\bar{U}_S = \frac{\omega A^2}{2\tanh(kH)} = \frac{gA^2}{2c}, \tag{5.3.2}$$

where we have utilized the dispersion relation (2.1.17). Similarly, for the Stokes flux in Sverdrup waves, (5.2.4) yields that

$$\bar{U}_S = \frac{cA^2}{2H}. \tag{5.3.3}$$

The energy densities for the two cases are given by (2.5.4) and (3.4.3), i.e. $E = \frac{1}{2}\rho_0 g A^2$ and $E = \frac{c^2 \rho_0 A^2}{2H}$, where we have utilized that $c_0^2 = gH$ for Sverdrup waves. We then see right away from (5.3.2) and (5.3.3) that for both cases we have the relation

$$E = c\rho_0 \bar{U}_S, \tag{5.3.4}$$

where $c = \omega / k$. Although we have here only demonstrated this relation for two types of waves, the fact that the energy density is equal to the total mean wave momentum times the phase speed is valid for a wide class of waves (Starr, 1959).

5.4 The mean Eulerian volume flux in shallow-water waves

By integrating (5.1.7) between the bottom and the free surface, and then average, we find that

$$\begin{aligned} \overline{U}_L &= \overline{U}_E + \overline{U}_S, \\ \overline{V}_L &= \overline{V}_E + \overline{V}_S. \end{aligned} \tag{5.4.1}$$

The Stokes drift (5.1.9) is a feature that is inherent in the periodic wave motion, and is basically independent of friction. The mean Eulerian current, on the other hand, is very much dependent on friction. As we have shown, it is fairly easy to compute the Stokes drift, while it is more difficult to determine the mean Eulerian current due to waves. We shall here be content by computing the mean Eulerian volume fluxes.

We have already derived exact expression for the Lagrangian volume fluxes, e.g. (1.2.3) and (1.2.6). For the discussion of the Eulerian fluxes we simplify, and take that we can apply the hydrostatic approximation in an ocean of constant depth. Furthermore, we apply a friction force of the type (1.1.8), and assume that there is no forcing from the wind or the air pressure at the surface. To second order in wave amplitude (1.2.6) then reduces to

$$\begin{aligned} \overline{U}_{Et} - f\overline{V}_E &= f\overline{V}_S - gH\overline{\eta}_x - g\overline{\eta\eta}_x - \left(\int_{-H}^{0} \overline{u^2} dz \right)_x - \left(\int_{-H}^{0} \overline{vu} dz \right)_y - \overline{\tau}_B^{(x)} / \rho_0, \\ \overline{V}_{Et} + f\overline{U}_E &= -f\overline{U}_S - gH\overline{\eta}_y - g\overline{\eta\eta}_y - \left(\int_{-H}^{0} \overline{uv} dz \right)_x - \left(\int_{-H}^{0} \overline{v^2} dz \right)_y - \overline{\tau}_B^{(y)} / \rho_0, \end{aligned} \tag{5.4.2}$$

Here we have utilized (5.4.1), and assumed that the Stokes flux is independent of time. The main problem here is to determine the bottom drag on the Eulerian flow. To simplify, we use a drag that is linear in the Eulerian fluxes, e.g. (1.5.4):

$$\bar{\tau}_B^{(x)} = \rho_0 K \overline{U}_E, \quad \bar{\tau}_B^{(y)} = \rho_0 K \overline{V}_E . \tag{5.4.3}$$

Here K is a constant bottom friction coefficient. It is in general different from the friction coefficient r in (3.5.13) that acts to dampen the linear waves, but we take that they are of the same order of magnitude.

We consider steady mean flow. In this case (5.4.2), (5.4.3) and (1.2.3) reduce to

$$\begin{aligned}
&- f\overline{V}_E + K\overline{U}_E + gH\overline{\eta}_x = f\overline{V}_S - g\overline{\eta\eta_x} - \left(\int_{-H}^{0} \overline{u^2} dz\right)_x - \left(\int_{-H}^{0} \overline{vu} dz\right)_y , \\
&f\overline{U}_E + K\overline{V}_E + gH\overline{\eta}_y = -f\overline{U}_S - g\overline{\eta\eta_y} - \left(\int_{-H}^{0} \overline{uv} dz\right)_x - \left(\int_{-H}^{0} \overline{v^2} dz\right)_y , \\
&\overline{U}_{Ex} + \overline{V}_{Ey} = -\overline{U}_{Sx} - \overline{V}_{Sy}.
\end{aligned} \tag{5.4.4}$$

The accuracy in this calculation of the mean fluxes is $O(A^2)$. To this order all the quantities on the right-hand side of (5.4.4) are completely determined from linear wave theory. Hence, (5.4.4) constitutes three inhomogeneous equations for determining the three unknowns $\overline{U}_E, \overline{V}_E, \overline{\eta}$. Appropriate boundary conditions must be added for the specific problem in question.

5.5 Application to transport in coastal Kelvin waves

Radiation stress

Since we already have considered the effect of friction on coastal Kelvin waves, e.g., Section 3.5, we have all the information we need to proceed, and calculate the mean Eulerian volume fluxes to $O(A^2)$ associated with this type of wave. For coastal Kelvin waves u is independent of z, $v = 0$, and $\overline{V}_S = 0$. Hence, from (5.4.4):

$$
\begin{aligned}
&-f\overline{V}_E + K\overline{U}_E + gH\overline{\eta}_x = -g\overline{\eta\eta}_x - 2H\overline{uu}_x,\\
&f\overline{U}_E + K\overline{V}_E + gH\overline{\eta}_y = -f\overline{U}_S - g\overline{\eta\eta}_y,\\
&\overline{U}_{Ex} + \overline{V}_{Ey} = -\overline{U}_{Sx}.
\end{aligned}
\tag{5.5.1}
$$

From (3.5.21) we easily obtain (use that $\alpha^2 << k^2$) for the non-linear terms on the right-hand side of (5.5.1):

$$
R_1 \equiv -g\overline{\eta\eta}_x - 2H\overline{uu}_x = \frac{3}{2}\alpha g A^2 \exp(-2\alpha x - 2y/a), \tag{5.5.2}
$$

$$
R_2 \equiv -g\overline{\eta\eta}_y = \frac{gA^2}{2a}\exp(-2\alpha x - 2y/a). \tag{5.5.3}
$$

Here R_1 and R_2 are referred to as wave-forcing terms since they arise from the periodic wave motion, and act on the mean flow. The Stokes flux (5.3.1) for this problem is easily computed. We obtain

$$
\overline{U}_S = \frac{c_0 A^2}{2H}\exp(-2\alpha x - 2y/a). \tag{5.5.4}
$$

We then realize that the wave-forcing terms R_1 and R_2 can be written:

$$
R_1 = -\frac{\partial}{\partial x}\left(\frac{3}{2}c_0\overline{U}_S\right), \tag{5.5.5}
$$

$$
R_2 = -\frac{\partial}{\partial y}\left(\frac{1}{2}c_0\overline{U}_S\right). \tag{5.5.6}
$$

The terms $3c_0\overline{U}_S/2$ and $c_0\overline{U}_S/2$ in (5.5.5) and (5.5.6) are known as the *radiation stress* components per unit density in shallow-water waves (Longuet-Higgins and Stewart, 1962). Actually, Longuet-Higgins and Stewart defined the radiation stress components in terms of the wave energy density *E*. It can be shown here, as in (5.3.4), that $E/\rho_0 = c_0\overline{U}_S$. In vector form, the radiation stresses (5.5.5) and (5.5.6) in the *x*- and *y*-direction are given as the (negative) divergence of the radiation stress tensor. It

is important to note that the concept of radiation stresses here is related to spatially varying waves, and tends to accelerate the mean flow.

Mean Eulerian fluxes

By inserting for R_1 and R_2, using that we also can write $R_2 = f\overline{U}_S$, we obtain for the mean Eulerian fluxes that

$$-f\overline{V}_E + K\overline{U}_E + gH\overline{\eta}_x = -\frac{\partial}{\partial x}\left(\frac{3}{2}c_0\overline{U}_S\right), \tag{5.5.7}$$

$$f\overline{U}_E + K\overline{V}_E + gH\overline{\eta}_y = 0\,. \tag{5.5.8}$$

$$\overline{U}_{Ex} + \overline{V}_{Ey} = -\overline{U}_{Sx}\,. \tag{5.5.9}$$

From the curl of (5.5.7)-(5.5.8) we obtain, by using (5.5.9):

$$\overline{V}_{Ex} - \overline{U}_{Ey} = \frac{4f\alpha}{K}\overline{U}_S\,. \tag{5.5.10}$$

From the divergence of (5.5.7)-(5.5.8), using (5.5.10), we find for the mean surface elevation

$$\nabla_H^2\overline{\eta} = \frac{4\alpha}{a^2K}\left(1 - \frac{3c_0\alpha K}{2f^2} - \frac{K^2}{2f^2}\right)\overline{U}_S\,. \tag{5.5.11}$$

We introduce the damping scale L of the waves by $L = 1/\alpha$. Furthermore we introduce the wave friction coefficient $r = 2c_0\alpha$ from (3.5.18). A particular solution of (5.5.11) can then be written

$$\overline{\eta} = \frac{r}{2c_0K(1 + a^2/L^2)}\left(1 - \frac{3rK}{4f^2} - \frac{K^2}{2f^2}\right)\overline{U}_S\,. \tag{5.5.12}$$

We must have that the surface elevation and the elevation gradients are finite at infinity. Then, apart from an insignificant constant, (5.5.12) represents our full solution.

In this problem we assume that the frictional effect on the waves and on the mean flow is of the same order of magnitude, i.e. $O(r) \sim O(K)$. Furthermore, we assume that the wave-damping distance L in the x-direction is much larger than the Rossby radius, or

$$a^2 << L^2 . \tag{5.5.13}$$

Alternatively, these conditions can be written $r^2 \sim K^2 << f^2$. Under these circumstances the mean surface elevation (5.5.12) simplifies to

$$\overline{\eta} = \frac{r}{2c_0 K}\overline{U}_S . \tag{5.5.14}$$

From (5.5.7) and (5.5.8) we then obtain in this approximation:

$$\overline{U}_E = \frac{r}{K}\overline{U}_S . \tag{5.5.15}$$

We note that due to friction, we have an induced mean Eulerian flux which is of the same order as the Stokes flux. Accordingly, the total mean Lagrangian flux in this case becomes

$$\overline{U}_L = (1 + r/K)\overline{U}_S . \tag{5.5.16}$$

The mean wave-induced particle velocity along the coast then becomes

$$\overline{u}_L = \frac{\overline{U}_L}{H} = \left(1 + \frac{r}{K}\right)\frac{c_0 A^2}{2H^2}\exp(-2\alpha x - 2y/a) . \tag{5.5.17}$$

Since we have a Lagrangian flux that decays along the coast, the flow field must be divergent, i.e. we must have that $\overline{V}_{Ly} = \overline{V}_{Ey} \neq 0$. More precisely, from (5.5.9) and (5.5.16) we obtain

$$\overline{V}_{Ey} = 2\alpha\left(1 + \frac{r}{K}\right)\overline{U}_S . \tag{5.5.18}$$

By integrating, and assuming that $V_E(y = 0) = 0$ (no flux normal to the coast), we obtain

$$\overline{V}_E = \frac{a}{L}\left(1+\frac{r}{K}\right)\left(\overline{U}_{S0} - \overline{U}_S\right), \tag{5.5.19}$$

where $\overline{U}_{S0}$ is the value of the Stokes flux at the coast, and $L = 1/\alpha$. This means that we have a small flux $\overline{V}_E$ which is directed in the positive *y*-direction. It has its maximum value *outside* the wave-trapped region (mathematically for $y \to \infty$, but in practice for $y \geq a$). By returning to (5.5.8), we note that with our adopted assumptions

$$\left|\frac{K\overline{V}_E}{f\overline{U}_E}\right| \sim \frac{K^2}{f^2} << 1. \tag{5.5.20}$$

This means that the along-shore Eulerian flux $\overline{U}_E$ in this case is approximately geostrophic.

We recall that our simplifications in this section rest on the assumption that the typical wave damping scale along the coast must be much larger than the Rossby radius. This could be fulfilled for tidally generated Kelvin waves on the wide and shallow Siberian shelf in the Polar Sea. It should also be noted this assumption is more easily fulfilled for internal Kelvin waves, since the internal Rossby radius is much smaller than the barotropic one. However, in this connection it must be pointed out that the damping scale for internal waves may be different from that of surface waves.

REFERENCES

Articles

Gill, A. E., and Clarke, A. J.: 1974, Deep-Sea Res., **21**, 325.

Longuet-Higgins, M. S., and Stewart, R. W.: 1962, J. Fluid Mech., **13**, 485.

Martinsen, E. A, Gjevik, B., and Røed, L. P.: 1979, J. Phys. Oceanogr., **9**, 1126.

Martinsen, E. A., and Weber, J. E.: 1981, Tellus, **33**, 402.

Starr, V. P.: 1959, Tellus, **11**, 135.

Stokes, G. G.: 1846, Rep. 16th Brit. Assoc. Adv. Sci., 1-20.

Stokes, G. G.: 1847, Trans. Cam. Phil. Soc., **8**, 441.

Sverdrup, H. U.: 1927, Geophys. Publ., **4**, 75.

Books

Defant, A.: 1961, Physical Oceanography, Vol. I & II. Pergamon Press, 1961.

Gill, A. E.: 1982, Atmosphere-Ocean Dynamics. Academic Press, 1982.

Krauss, W.: 1973, Methods and Results of Theoretical Oceanography, Vol. I.

Gebrüder Borntraeger, 1973.

LeBlond, P. H., and Mysak, L. A.: 1978, Waves in the Ocean. Elsevier, 1978.

Pedlosky, J.: 1987, Geophysical Fluid Dynamics, 2. ed. Springer, 1987.